References

1. Tangye SG, Deenick EK, Palendira U, Ma CS. T cell-B cell interactions in primary immunodeficiencies. *Ann N Y Acad Sci.* 2012;1250(1):1-13.
2. Breitfeld D, Ohl L, Kremmer E, et al. Follicular B helper T cells express CXC chemokine receptor 5, localize to B cell follicles, and support immunoglobulin production. *J Exp Med.* 2000;192(11): 1545-1552.
3. Schaerli P, Willimann K, Lang AB, Lipp M, Loetscher P, Moser B. CXC chemokine receptor 5 expression defines follicular homing T cells with B cell helper function. *J Exp Med.* 2000;192(11): 1553-1562.
4. Chtanova T, Tangye SG, Newton R, et al. T follicular helper cells express a distinctive transcriptional profile, reflecting their role as non-Th1/Th2 effector cells that provide help for B cells. *J Immunol.* 2004;173(1):68-78.
5. Yu D, Rao S, Tsai LM, et al. The transcriptional repressor Bcl-6 directs T follicular helper cell lineage commitment. *Immunity.* 2009;31(3):457-468.
6. Johnston RJ, Poholek AC, Ditoro D, et al. Bcl6 and Blimp-1 are reciprocal and antagonistic regulators of T follicular helper cell differentiation. *Science.* 2009;325(5943):1006-1010.
7. Nurieva RI, Chung Y, Martinez GJ, et al. Bcl6 mediates the development of T follicular helper cells. *Science.* 2009;325(5943):1001-1005.
8. Deenick EK, Ma CS. The regulation and role of T follicular helper cells in immunity. *Immunology.* 2011;134(4):361-367.
9. Ma CS, Deenick EK. The role of SAP and SLAM family molecules in the humoral immune response. *Ann N Y Acad Sci.* 2011;1217:32-44.
10. Rasheed A-U, Rahn H-P, Sallusto F, Lipp M, Müller G. Follicular B helper T cell activity is confined to CXCR5(hi)ICOS(hi) CD4 T cells and is independent of CD57 expression. *Eur J Immunol.* 2006;36(7):1892-1903.
11. Ma CS, Suryani S, Avery DT, et al. Early commitment of naive human CD4(+) T cells to the T follicular helper (T(FH)) cell lineage is induced by IL-12. *Immunol Cell Biol.* 2009;87(8):590-600.
12. Deenick EK, Ma CS, Brink R, Tangye SG. Regulation of T follicular helper cell formation and function by antigen presenting cells. *Curr Opin Immunol.* 2011;23(1):111-118.
13. Vogelzang A, McGuire HM, Yu D, Sprent J, Mackay CR, King C. A fundamental role for interleukin-21 in the generation of T follicular helper cells. *Immunity.* 2008;29(1):127-137.
14. Nurieva RI, Chung Y, Hwang D, et al. Generation of T follicular helper cells is mediated by interleukin-21 but independent of T helper 1, 2, or 17 cell lineages. *Immunity.* 2008;29(1):138-149.
15. Dienz O, Eaton SM, Bond JP, et al. The induction of antibody production by IL-6 is indirectly mediated by IL-21 produced by CD4+ T cells. *J Exp Med.* 2009;206(1):69-78.
16. Eddahri F, Denanglaire S, Bureau F, et al. Interleukin-6/STAT3 signaling regulates the ability of naive T cells to acquire B-cell help capacities. *Blood.* 2009;113(11):2426-2433.
17. Batten M, Ramamoorthi N, Kljavin NM, et al. IL-27 supports germinal center function by enhancing IL-21 production and the function of T follicular helper cells. *J Exp Med.* 2010;207(13): 2895-2906.
18. Poholek AC, Hansen K, Hernandez SG, et al. In vivo regulation of Bcl6 and T follicular helper cell development. *J Immunol.* 2010;185(1):313-326.
19. Eto D, Lao C, Ditoro D, et al. IL-21 and IL-6 are critical for different aspects of B cell immunity and redundantly induce optimal follicular helper CD4 T cell (Tfh) differentiation. *PLoS One.* 2011;6(3): e17739.
20. Leonard WJ. Cytokines and immunodeficiency diseases. *Nat Rev Immunol.* 2001;1(3):200-208.
21. Hibbert L, Pflanz S, De Waal Malefyt R, Kastelein RA. IL-27 and IFN-alpha signal via Stat1 and Stat3 and induce T-Bet and IL-12Rbeta2 in naive T cells. *J Interferon Cytokine Res.* 2003;23(9):513-522.
22. Schmitt N, Morita R, Bourdery L, et al. Human dendritic cells induce the differentiation of interleukin-21-producing T follicular helper-like cells through interleukin-12. *Immunity.* 2009;31(1):158-169.
23. Ma CS, Chew GYJ, Simpson N, et al. Deficiency of Th17 cells in hyper IgE syndrome due to mutations in STAT3. *J Exp Med.* 2008;205(7):1551-1557.
24. Avery DT, Deenick EK, Ma CS, et al. B cell-intrinsic signaling through IL-21 receptor and STAT3 is required for establishing long-lived antibody responses in humans. *J Exp Med.* 2010; 207(1):155-171.
25. Minegishi Y, Saito M, Morio T, et al. Human tyrosine kinase 2 deficiency reveals its requisite roles in multiple cytokine signals involved in innate and acquired immunity. *Immunity.* 2006; 25(5):745-755.
26. de Beaucoudrey L, Samarina A, Bustamante J, et al. Revisiting human IL-12Rbeta1 deficiency: a survey of 141 patients from 30 countries. *Medicine (Baltimore).* 2010;89(6):381-402.
27. Woellner C, Gertz EM, Schaffer AA, et al. Mutations in STAT3 and diagnostic guidelines for hyper-IgE syndrome. *J Allergy Clin Immunol.* 2010; 125(2):424-432 e428.
28. Kilic SS, Hacimustafaoglu M, Boisson-Dupuis S, et al. A patient with tyrosine kinase 2 deficiency without hyper-IgE syndrome [published online ahead of print March 6, 2012]. *J Pediatr.* doi: 10.1016/j.peds.2012.01.056.
29. Ma CS, Hare NJ, Nichols KE, et al. Impaired humoral immunity in X-linked lymphoproliferative disease is associated with defective IL-10 production by CD4+ T cells. *J Clin Invest.* 2005; 115(4):1049-1059.
30. Altare F, Durandy A, Lammas D, et al. Impairment of mycobacterial immunity in human interleukin-12 receptor deficiency. *Science.* 1998; 280(5368):1432-1435.
31. de Jong R, Altare F, Haagen IA, et al. Severe mycobacterial and Salmonella infections in interleukin-12 receptor-deficient patients. *Science.* 1998; 280(5368):1435-1438.
32. Parham C, Chirica M, Timans J, et al. A receptor for the heterodimeric cytokine IL-23 is composed of IL-12Rbeta1 and a novel cytokine receptor subunit, IL-23R. *J Immunol.* 2002;168(11):5699-5708.
33. Gollob JA, Veenstra KG, Jyonouchi H, et al. Impairment of STAT activation by IL-12 in a patient with atypical mycobacterial and staphylococcal infections. *J Immunol.* 2000;165(7):4120-4126.
34. Jacobson NG, Szabo SJ, Weber-Nordt RM, et al. Interleukin 12 signaling in T helper type 1 (Th1) cells involves tyrosine phosphorylation of signal transducer and activator of transcription (Stat)3 and Stat4. *J Exp Med.* 1995;181(5):1755-1762.
35. Bacon CM, Petricoin EF III, Ortaldo JR, et al. Interleukin 12 induces tyrosine phosphorylation and activation of STAT4 in human lymphocytes. *Proc Natl Acad Sci U S A.* 1995;92(16):7307-7311.
36. Minegishi Y, Saito M, Tsuchiya S, et al. Dominant-negative mutations in the DNA-binding domain of STAT3 cause hyper-IgE syndrome. *Nature.* 2007; 448(7157):1058-1062.
37. Holland SM, DeLeo FR, Elloumi HZ, et al. STAT3 mutations in the hyper-IgE syndrome. *N Engl J Med.* 2007;357(16):1608-1619.
38. Bacon CM, McVicar DW, Ortaldo JR, Rees RC, O'Shea JJ, Johnston JA. Interleukin 12 (IL-12) induces tyrosine phosphorylation of JAK2 and TYK2: differential use of Janus family tyrosine kinases by IL-2 and IL-12. *J Exp Med.* 1995; 181(1):399-404.
39. Watford WT, O'Shea JJ. Human tyk2 kinase deficiency: another primary immunodeficiency syndrome. *Immunity.* 2006;25(5):695-697.
40. Kubin M, Kamoun M, Trinchieri G. Interleukin 12 synergizes with B7/CD28 interaction in inducing efficient proliferation and cytokine production of human T cells. *J Exp Med.* 1994;180(1):211-222.
41. Gett AV, Hodgkin PD. Cell division regulates the T cell cytokine repertoire, revealing a mechanism underlying immune class regulation. *Proc Natl Acad Sci U S A.* 1998;95(16):9488-9493.
42. Nakayamada S, Kanno Y, Takahashi H, et al. Early Th1 cell differentiation is marked by a Tfh cell-like transition. *Immunity.* 2011;35(6):919-931.
43. Wei L, Laurence A, Elias KM, O'Shea JJ. IL-21 is produced by Th17 cells and drives IL-17 production in a STAT3-dependent manner. *J Biol Chem.* 2007;282(48):34605-34610.
44. Wei L, Vahedi G, Sun HW, et al. Discrete roles of STAT4 and STAT6 transcription factors in tuning epigenetic modifications and transcription during T helper cell differentiation. *Immunity.* 2010;32(6): 840-851.
45. Akiba H, Takeda K, Kojima Y, et al. The role of ICOS in the CXCR5+ follicular B helper T cell maintenance in vivo. *J Immunol.* 2005;175(4): 2340-2348.
46. Choi YS, Kageyama R, Eto D, et al. ICOS receptor instructs T follicular helper cell versus effector cell differentiation via induction of the transcriptional repressor Bcl6. *Immunity.* 2011;34(6):932-946.
47. Speckmann C, Enders A, Woellner C, et al. Reduced memory B cells in patients with hyper IgE syndrome. *Clin Immunol.* 2008;129(3):448-454.
48. Sheerin KA, Buckley RH. Antibody responses to protein, polysaccharide, and phi X174 antigens in the hyperimmunoglobulinemia E (hyper-IgE) syndrome. *J Allergy Clin Immunol.* 1991;87(4):803-811.
49. Yong PF, Salzer U, Grimbacher B. The role of costimulation in antibody deficiencies: ICOS and common variable immunodeficiency. *Immunol Rev.* 2009;229(1):101-113.
50. Al-Herz W, Bousfiha A, Casanova J-L, et al. Primary immunodeficiency diseases: an update on the classification from the International Union of Immunological Societies Expert Committee for Primary Immunodeficiency. *Front Immunol.* 2011; 2:1-26.

Please cite this article in press as: Wakabayashi et al., Impaired KLHL3-Mediated Ubiquitination of WNK4 Causes Human Hypertension, Cell Reports (2013), http://dx.doi.org/10.1016/j.celrep.2013.02.024

Cell Reports
Article

Open ACCESS

Impaired KLHL3-Mediated Ubiquitination of WNK4 Causes Human Hypertension

Mai Wakabayashi,[1,4] Takayasu Mori,[1,4] Kiyoshi Isobe,[1] Eisei Sohara,[1] Koichiro Susa,[1] Yuya Araki,[1] Motoko Chiga,[1] Eriko Kikuchi,[1] Naohiro Nomura,[1] Yutaro Mori,[1] Hiroshi Matsuo,[2] Tomohiro Murata,[2] Shinsuke Nomura,[2] Takako Asano,[3] Hiroyuki Kawaguchi,[3] Shigeaki Nonoyama,[3] Tatemitsu Rai,[1] Sei Sasaki,[1] and Shinichi Uchida[1,*]

[1]Department of Nephrology, Graduate Schools of Medical and Dental Sciences, Tokyo Medical and Dental University, 1-5-45 Yushima, Bunkyo, Tokyo 113-8519, Japan

[2]Department of Cardiology and Nephrology, Mie University Graduate School of Medicine, 2-174 Edobashi, Tsu, Mie 514-8507, Japan

[3]Department of Pediatrics, National Defense Medical College, 3-2 Namiki, Tokorozawa, Saitama 359-8513, Japan

[4]These authors contributed equally to this work

*Correspondence: suchida.kid@tmd.ac.jp

http://dx.doi.org/10.1016/j.celrep.2013.02.024

SUMMARY

Mutations in WNK kinases cause the human hypertensive disease pseudohypoaldosteronism type II (PHAII), but the regulatory mechanisms of the WNK kinases are not well understood. Mutations in kelch-like 3 (*KLHL3*) and *Cullin3* were also recently identified as causing PHAII. Therefore, new insights into the mechanisms of human hypertension can be gained by determining how these components interact and how they are involved in the pathogenesis of PHAII. Here, we found that KLHL3 interacted with Cullin3 and WNK4, induced WNK4 ubiquitination, and reduced the WNK4 protein level. The reduced interaction of KLHL3 and WNK4 by PHAII-causing mutations in either protein reduced the ubiquitination of WNK4, resulting in an increased level of WNK4 protein. Transgenic mice overexpressing WNK4 showed PHAII phenotypes, and WNK4 protein was indeed increased in *Wnk4*$^{D561A/+}$ PHAII model mice. Thus, WNK4 is a target for KLHL3-mediated ubiquitination, and the impaired ubiquitination of WNK4 is a common mechanism of human hereditary hypertension.

INTRODUCTION

Hypertension is one of the biggest health problems in the industrialized world because it damages critical organs. Studies of monogenic hypertensive diseases, such as Liddle syndrome (Shimkets et al., 1994) and pseudohypoaldosteronism type II (PHAII) (Achard et al., 2001), have provided new insight into the mechanisms of blood pressure regulation in humans. Liddle syndrome is caused by mutations in the epithelial sodium channel (ENaC) that increase the amount of ENaC in the apical membranes of collecting ducts in the kidney through the impairment of ENaC ubiquitination, thereby increasing sodium reabsorption (Rossier and Schild, 2008). PHAII is another autosomal-dominant hereditary hypertensive disease that is characterized by hyperkalemia and metabolic acidosis (Gordon, 1986), and genes encoding the WNK kinases (WNK1 and WNK4) were identified in 2001 as responsible (Wilson et al., 2001). However, the pathogenesis of PHAII was totally unknown when the WNK genes were identified. Since then, numerous in vitro and in vivo studies have been performed for clarifying the molecular pathogenesis of PHAII (Bergaya et al., 2011; Lalioti et al., 2006; Liu et al., 2011; McCormick and Ellison, 2011; Yang et al., 2003). We generated a mouse model of PHAII carrying the same mutation as patients with PHAII (*Wnk4*$^{D561A/+}$ knockin mouse) (Yang et al., 2007) and discovered that the constitutive activation of a novel signal cascade, consisting of WNK kinases, OSR1 and SPAK kinases, and the Na-Cl cotransporter (NCC), is the major pathogenic mechanism of PHAII (Chiga et al., 2008, 2011). However, the molecular pathogenesis of how the missense mutation of WNK4 activates the cascade remains to be clarified.

Recently, two new genes (*KLHL3* and *Cullin3*) were also identified as being associated with PHAII (Boyden et al., 2012; Louis-Dit-Picard et al., 2012). However, how these genes are involved in PHAII is unknown. Determining how these responsible genes (*WNK*, *KLHL3*, and *Cullin3*) are orchestrated and how pathogenic mutations in these genes cause a common hypertensive disease will contribute to the understanding of the molecular pathogenesis of human hypertension and also to the identification of new targets for antihypertensive drugs.

The purpose of the present study was to determine the pathogenic role of PHAII-causing mutations in the *WNK4*, *KLHL3*, and *Cullin3* genes. We found that WNK4 kinase is a substrate of KLHL3-Cullin3-targeted ubiquitination and that the PHAII-causing mutations of *WNK4* and *KLHL3* resulted in impaired WNK4 ubiquitination. The resultant increase in the WNK4 level was confirmed in *Wnk4*$^{D561A/+}$ PHAII model mice; this increase constitutively activates the WNK-OSR1/SPAK-NCC signal cascade and causes PHAII. Data from *WNK4* transgenic mice were consistent with this idea.

RESULTS

KLHL3 Interacted with and Regulated the Abundance of WNK4 Kinase Protein

We have reported that the activation of the WNK-OSR1/SPAK-NCC signal cascade is the major pathogenic mechanism of PHAII caused by a *WNK4* mutation (Yang et al., 2007), and

Please cite this article in press as: Wakabayashi et al., Impaired KLHL3-Mediated Ubiquitination of WNK4 Causes Human Hypertension, Cell Reports (2013), http://dx.doi.org/10.1016/j.celrep.2013.02.024

Cell PRESS
Open ACCESS

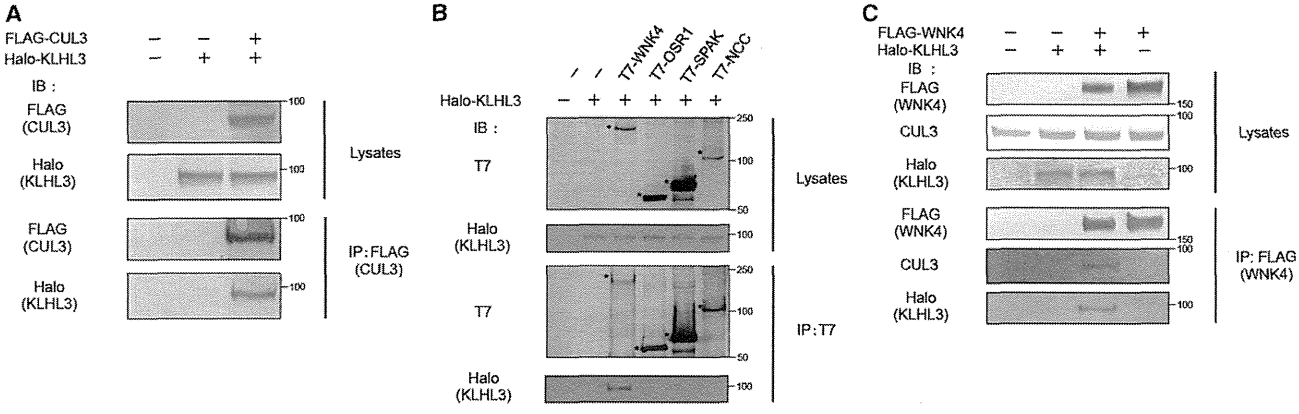

Figure 1. KLHL3 Was Coimmunoprecipitated with Cullin3 and WNK4

(A) FLAG-tagged Cullin3 (CUL3) was coimmunoprecipitated with Halo-tagged KLHL3 in HEK293T cells. IB, immunoblot; IP, immunoprecipitation.

(B) T7-tagged WNK4, OSR1, SPAK, and NCC were coexpressed with Halo-tagged KLHL3 in HEK293T cells and immunoprecipitated with T7 antibody. KLHL3 was coimmunoprecipitated only with WNK4. The asterisks indicate T7-tagged proteins.

(C) WNK4 was coimmunoprecipitated with endogenous Cullin3 in HEK293T cells in the presence of KLHL3 coexpression. Results similar to those shown in (A), (B), and (C) were obtained in three separate experiments.

mutations in the *KLHL3* and *Cullin3* genes were also reported as causing the same PHAII phenotypes (Boyden et al., 2012; Louis-Dit-Picard et al., 2012). These data suggest that KLHL3 and Cullin3 may somehow interact with the components of the WNK-OSR1/SPAK-NCC signal cascade. Because KLHL proteins function as substrate adaptors in Cullin3-based E3 ligase (Cirak et al., 2010; Kigoshi et al., 2011; Lee et al., 2010; Lin et al., 2011), we first confirmed a complex formation of KLHL3 and Cullin3 via coimmunoprecipitation (Figure 1A). We then investigated whether KLHL3 interacted with the components of the WNK-OSR1/SPAK-NCC signal cascade. To verify this, we performed coimmunoprecipitation assays of KLHL3 with WNK4, OSR1, SPAK, and NCC. As shown in Figure 1B, KLHL3 was coimmunoprecipitated with WNK4, but not with OSR1, SPAK, or NCC. The interaction of Cullin3 with WNK4 was also confirmed through coimmunoprecipitation when KLHL3 was overexpressed (Figure 1C), consistent with the previously reported role of KLHL proteins as substrate adaptors in the Cullin3-based ubiquitin E3 ligase (Cirak et al., 2010; Kigoshi et al., 2011; Lee et al., 2010; Lin et al., 2011). We tried to demonstrate coimmunoprecipitation of endogenous WNK4 and KLHL3 in kidney tissue and in cultured cells. However, this was not successful due to the relatively low level of expression of WNK4 in cultured cells and the lack of KLHL3 antibodies adequate for immunoprecipitation. The finding that WNK4 might be readily degraded by the binding to KLHL3 within cells as shown below also made the detection of coimmunoprecipitation difficult, especially in kidney samples.

To clarify the functional role of KLHL3 on WNK4, we overexpressed KLHL3 along with WNK4. As shown in Figure 2A, KLHL3 overexpression dramatically decreased WNK4 protein expression, even when overexpressed by a strong cytomegalovirus (CMV) promoter. The expression level of bacterial alkaline phosphatase (BAP) driven by the same promoter was not affected by KLHL3 coexpression. OSR1, SPAK, and NCC expression levels were also not affected by KLHL3 coexpression (Figure 2B), supporting the results from the coimmunoprecipitation. To confirm the effect of KLHL3 on WNK4, we evaluated this effect on the endogenous WNK4 in mpkDCT cells, a mouse distal-tubule-derived cell line (Duong Van Huyen et al., 2001) (Figure 2C). Wild-type KLHL3 significantly decreased the endogenous WNK4 protein level. Conversely, KLHL3 knockdown significantly increased the WNK4 protein level (Figure 2D). Although these effects of KLHL3 expression on WNK4 were observed without Cullin3 overexpression, we further tested the effect of Cullin3 overexpression on WNK4 in human embryonic kidney 293T (HEK293T) cells. As shown in Figure 2E, coexpression of Cullin3 with KLHL3 further decreased the WNK4 protein level compared with the expression of KLHL3 alone. Cullin3 alone did not affect WNK4 abundance. These data suggested that the KLHL3-Cullin3 complex might be a strong regulator of the WNK4 protein abundance within cells. Although we tried to measure the half-life of WNK4 in the presence of KLHL3 and Cullin3, the robust decrease of WNK4 by KLHL3 and Cullin3 made the measurement extremely difficult. The difference could be highly significant based on the steady-state levels of transiently expressed WNK4, as shown in Figures 2A and 2B.

Next, we evaluated how a PHAII-causing mutation (R528H) of KLHL3 and Cullin3 affected the abundance of WNK4. When the expression levels of wild-type and mutant KLHL3 were similar, the R528H mutant was less able to reduce the endogenous protein level of WNK4 as compared to wild-type KLHL3 (Figure 2C). The PHAII-causing mutations of the *Cullin3* gene were reported to cause skipping of exon 9, which codes the segment (57 residues from 403–459) linking the BTB-binding and RING-binding domains of Cullin3 (Boyden et al., 2012). To investigate the pathogenic effect of the mutant Cullin3, we prepared Cullin3 lacking this segment. As shown in Figure 2E, the mutant Cullin3 was also less able to reduce WNK4 as compared to wild-type Cullin3.

Please cite this article in press as: Wakabayashi et al., Impaired KLHL3-Mediated Ubiquitination of WNK4 Causes Human Hypertension, Cell Reports (2013), http://dx.doi.org/10.1016/j.celrep.2013.02.024

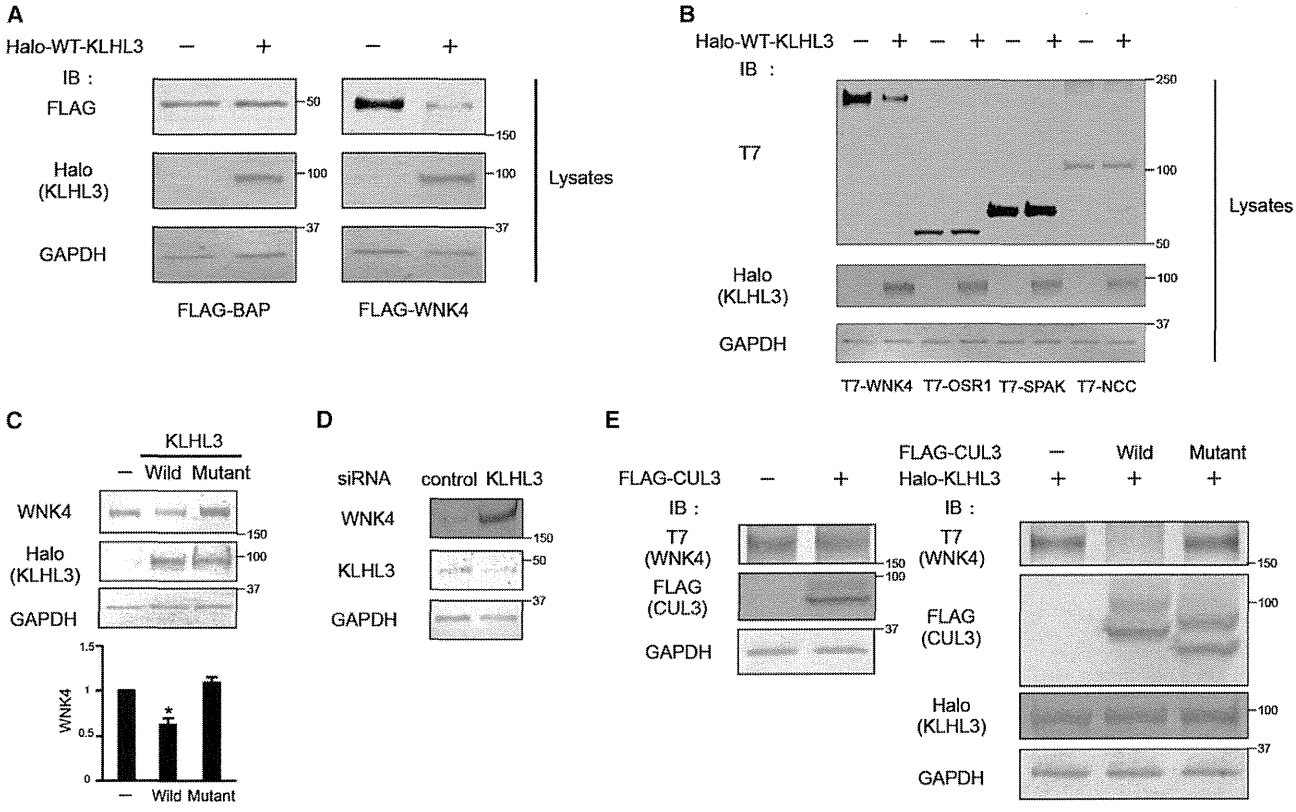

Figure 2. Effect of Wild-Type and PHAII-Causing Mutant KLHL3 and Cullin3 Expression on Cellular WNK4 Abundance

(A) When coexpressed with KLHL3, the abundance of WNK4 protein within HEK293T cells expressed by CMV promoter (p3×FLAG-CMV-10 vector, Sigma-Aldrich) was dramatically decreased, whereas the abundance of BAP expressed by the same expression vector was not affected by KLHL3 coexpression.

(B) The reduction of WNK4 by KLHL3 coexpression was confirmed in another expression system of WNK4 (pRK5 vector), and OSR1, SPAK, and NCC levels were not affected by KLHL3 coexpression. Results similar to those shown in (A) and (B) were obtained in three separate experiments.

(C) Effect of wild-type and a PHAII-causing mutant (R528H) KLHL3 expression on the cellular abundance of WNK4. Endogenous WNK4 level in mpkDCT cells was decreased by wild-type KLHL3 expression. However, a similar level of the mutant KLHL3 expression failed to reduce WNK4 (*$p < 0.05$, compared with the WNK4 levels without KLHL3 coexpression [left lane] and with the mutant KLHL3 coexpression [right lane]; n = 3; mean ± SEM).

(D) Effect of the endogenous KLHL3 knockdown in mpkDCT cells on WNK4 expression. The protein levels of WNK4 were higher in KLHL3-knocked-down cells than in control cells. siRNA, small interfering RNA.

(E) Effect of wild-type and a PHAII-causing mutant *Cullin3* expression on the cellular abundance of WNK4. Although the expression of Cullin3 alone did not affect WNK4 protein level, Cullin3 expression with KLHL3 dramatically reduced WNK4 protein. The mutant *Cullin3* lacking the portion corresponding to exon 9 was less able to reduce WNK4 protein. The existence of two bands in the immunoblot of Cullin3 was reported previously (McEvoy et al., 2007). Similar results were obtained in three separate experiments.

PHAII-Causing Mutations of *WNK4* and *KLHL3* Affected the Interaction of WNK4 and KLHL3 and the Ubiquitination of WNK4

To investigate the mechanism(s) by which KLHL3 regulates the WNK4 protein level, we examined the ubiquitination of wild-type and PHAII-causing WNK4 with or without wild-type and mutant KLHL3. In this assay, we did not overexpress Cullin3, but used endogenous Cullin3 in HEK 293T cells (Figure 1C) because the overexpression of Cullin3 with KLHL3 robustly decreased WNK4 protein abundance (Figure 2E) under our experimental conditions, even in the presence of proteasome inhibitors, which made it difficult to recover WNK4 for immunoprecipitation. After coexpression of FLAG-tagged WNK4, Halo-tagged KLHL3, and hemagglutinin (HA)-tagged ubiquitin in HEK293T cells, the cells were treated with 1 μM epoxomicin, and WNK4 was immunoprecipitated with FLAG antibody. First, we evaluated whether KLHL3 expression increased WNK4 ubiquitination. For the exclusion of ubiquitination signals from other proteins coimmunoprecipitated with WNK4, the immunoprecipitation was performed under a denaturing condition (Figure 3A). As previously shown in Figures 2A and 2B, when we expressed the wild-type KLHL3, the level of coexpressed wild-type WNK4 decreased significantly, even in the presence of a potent proteasome inhibitor (see WNK4 immunoblots of lysates and immunoprecipitated products in Figures 3A and 3C). As shown in the ubiquitin (HA) immunoblot (Figure 3A), the ubiquitination signals were observed as a smear band of over 200 kDa, which is the apparent molecular size of WNK4 (arrow). This data strongly suggested that WNK4 itself was indeed ubiquitinated, given that the immunoprecipitation was performed

Please cite this article in press as: Wakabayashi et al., Impaired KLHL3-Mediated Ubiquitination of WNK4 Causes Human Hypertension, Cell Reports (2013), http://dx.doi.org/10.1016/j.celrep.2013.02.024

Cell PRESS
Open ACCESS

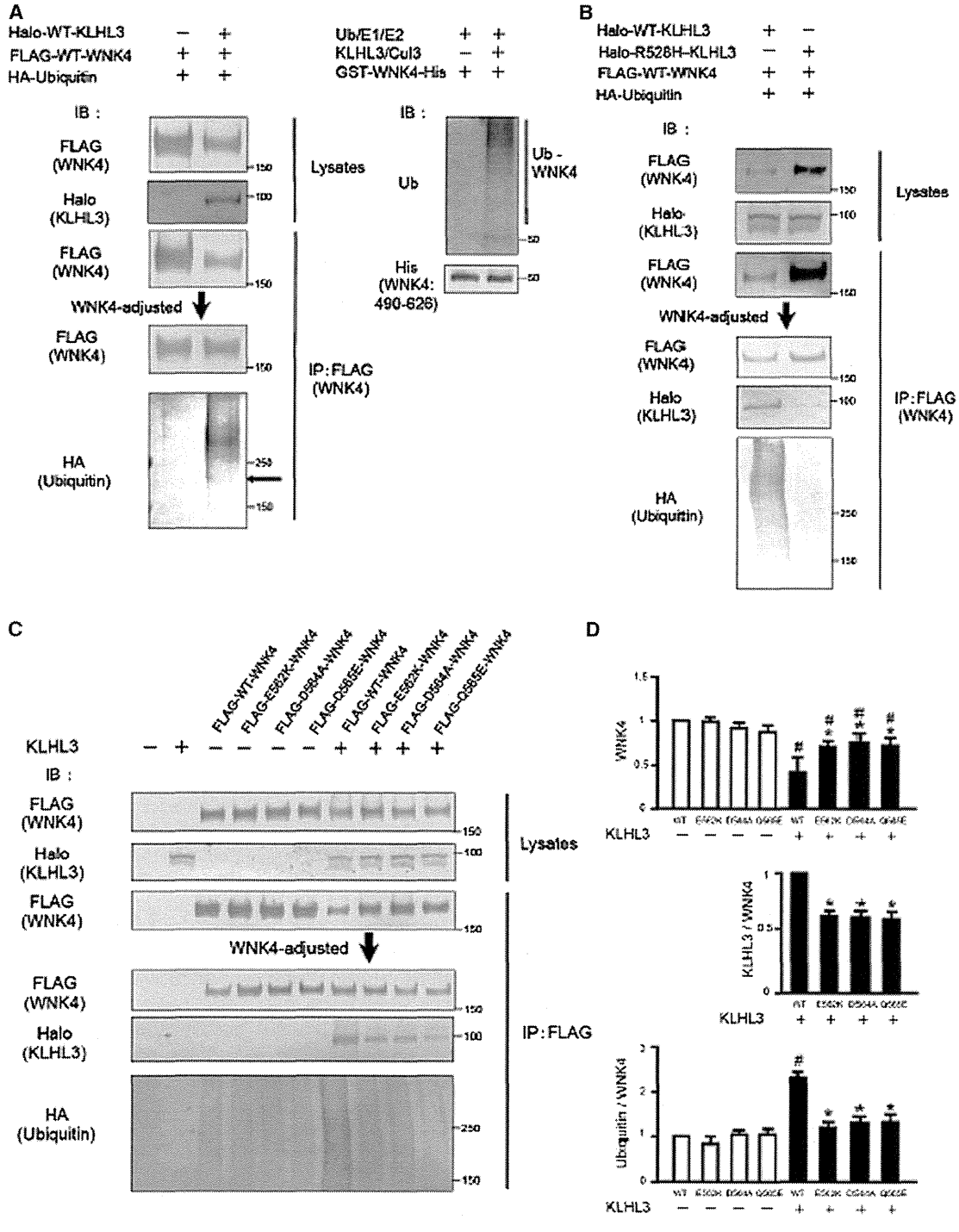

Figure 3. Effect of KLHL3 on the Ubiquitination of Wild-Type and PHAII-Causing Mutant WNK4

(A) Left panels: KLHL3 coexpression significantly induced the ubiquitination of wild-type WNK4. WNK4 was immunoprecipitated under a denaturing condition, and ubiquitinated WNK4 was observed as a smear band over 200 kDa, which is the apparent molecular size of WNK4 (arrow). Coexpression of wild-type KLHL3 significantly reduced the wild-type WNK4 level, even in the presence of 1 μM epoxomicin. Accordingly, in the lower panels, we reloaded the immunoprecipitated WNK4 samples to have equal amounts of immunoprecipitated WNK4 in each lane to demonstrate the difference in ubiquitination in each lane more clearly. We confirmed in the preliminary experiments that the data after loading adjustment faithfully reflected the data corrected by the immunoprecipitated WNK4 abundance before adjustment.

Right panels: In vitro ubiquitination assay of WNK4. WNK4 (490–626; 50 kDa) was incubated with ubiquitin, E1, and E2 (UbcH5a/UBE2D1) with or without the Cullin3-KLHL3 complex. Cullin3-KLHL3 significantly ubiquitinated WNK4 (490–626) in vitro. Similar results were obtained in three separate experiments.

(legend continued on next page)

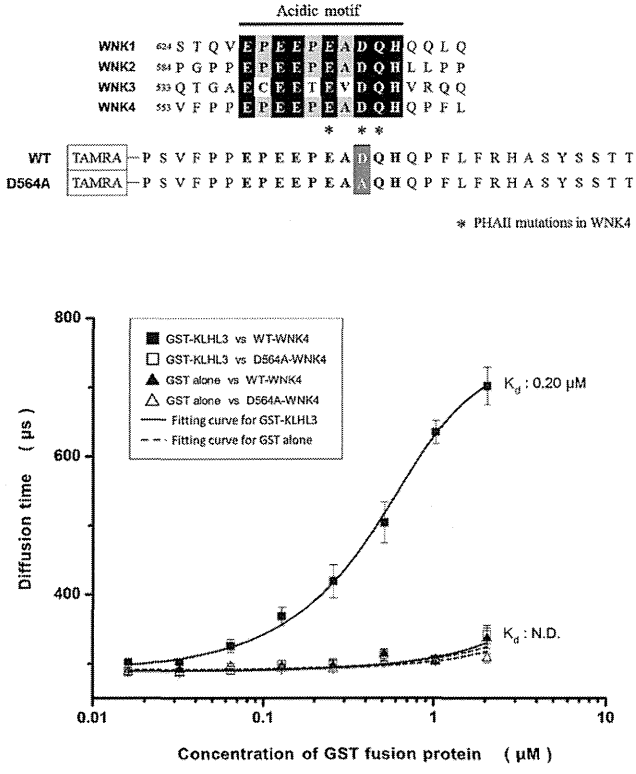

Figure 4. Direct Binding of KLHL3 to the Acidic Motif of Wild-Type WNK4

The diffusion time of a single-molecule TAMRA-labeled peptide corresponding to the acidic domain of wild-type WNK4 was measured by FCS. The addition of GST-KLHL3, not of GST only, dose-dependently increased the diffusion time, indicating the direct binding of KLHL3 to the acidic domain of WNK4 (K_d = 0.20 μM). The diffusion time of a TAMRA-labeled peptide carrying a PHAII-causing mutation (D564A) was not affected by the addition of GST-KLHL3. The results are presented as means ± SEM (n = 5). N.D., not determined.

under a denaturing condition. This ubiquitination was apparently increased by KLHL3 coexpression when the ubiquitination signals were corrected by the immunoprecipitated WNK4 abundance. To make the difference clear without correction, we adjusted the loading amount of the immunoprecipitated product to have the same amount of immunoprecipitated WNK4 in each lane in Figure 3A. A significant increase of WNK4 ubiquitination by KLHL3 was observed.

To further confirm that WNK4 was directly ubiquitinated by the KLHL3-Cullin3 complex, we performed an in vitro ubiquitination assay. Because the preparation of whole WNK4 protein was not successful, we prepared a portion of human WNK4 protein (residues from 490 to 626) containing the PHAII mutation sites as a GST fusion protein with a C-terminal His tag (50 kDa). As shown in the right panels of Figure 3A, we could confirm that the KLHL3-Cullin3 complex was able to directly ubiquitinate WNK4 (490–626).

Second, we tested the effect of the R528H KLHL3 mutation on WNK4 binding and ubiquitination. As already shown in Figure 2C, coexpression of wild-type KLHL3 significantly reduced WNK4 expression as compared with the mutant KLHL3 (Figure 3B, upper three panels). We observed a significant decrease in WNK4 ubiquitination by the mutant KLHL3 and also the decreased interaction of WNK4 with the mutant KLHL3 (Figure 3B, lower three panels).

We also tested the effect of PHAII-causing mutations of *WNK4* on WNK4-KLHL3 interaction and WNK4 ubiquitination. As shown in Figure 3A, wild-type KLHL3 decreased WNK4. However, this decrease mediated by KLHL3 was blunted in all three PHAII-causing *WNK4* mutants (Figure 3C, upper WNK4 panels). In the lower panels of Figure 3C, we showed the immnoblots of coimunoprecitated KLHL3 and ubiquitinated WNK4 after the loading adjustment as shown in Figures 3A and 3B. At the same time, we measured the signals before the loading adjustment and corrected the levels of WNK4 abundance as shown in Figure 3D. In either analysis, we could observe that the WNK4 mutants appeared to show less interaction with wild-type KLHL3 and less ubiquitination compared with wild-type WNK4. An in vitro ubiquitination assay using the wild-type and the mutant (D564A) WNK4 also supported this data (Figure S1).

The above data suggested that the acidic domain of WNK kinases (Figure 4), where PHAII mutants were clustered in WNK4, might be involved in the interaction with KLHL3. To investigate this hypothesis and to clarify whether the interaction of WNK4 and KLHL3 was direct, we measured the binding of TAMRA-labeled WNK4 peptide covering the acidic motif to the whole KLHL3 protein as a GST fusion protein in vitro. We used fluorescence correlation spectroscopy (FCS) to measure the diffusion time of the fluorescent peptide (FluoroPoint-Light,

(B) Effect of wild-type and a PHAII-causing mutant KLHL3 expression on WNK4-KLHL3 binding and WNK4 ubiquitination. Upper panels: as shown in Figure 2C, wild-type KLHL3 reduced the coexpressed WNK4 protein level more significantly than did the mutant KLHL3, even in the presence of 1 μM epoxomicin. Accordingly, as in Figure 3A, the immunoprecipitated WNK4 samples were reloaded for equal amounts of immunoprecipitated WNK4 in each lane (lower panels). The binding of WNK4 to mutant KLHL3 and WNK4 ubiquitination by the mutant KLHL3 were significantly impaired. The immunoprecipitation was performed under a nondenaturing condition for assessing the binding to KLHL3 in the same experiments. Similar results were obtained in three separate experiments.

(C) Effect of PHAII-causing mutations of *WNK4* on WNK4-KLHL3 binding and WNK4 ubiquitination. As shown in Figure 3A, coexpression of wild-type KLHL3 significantly reduced the wild-type WNK4 level, even in the presence of 1 μM epoxomicin. However, this decrease was blunted in PHAII-causing *WNK4* mutations (see WNK4 immunoblots of lysates or immunoprecipitates in the upper panels). All three PHAII-causing WNK4 mutants showed less ubiquitination and less binding to KLHL3 (see quantification of blots in D).

(D) Quantification of the results showing the comparison of WNK4 ubiquitination and WNK4 binding to KLHL3 among wild-type and PHAII-causing WNK4 mutants. Upper graph, immunoprecipitated WNK4 abundance; middle graph, coimmunoprecipitated KLHL3 corrected by WNK4 abundance; lower graph, WNK4 ubiquitination corrected by WNK4 abundance. WNK4 ubiquitination was evaluated by separate sets of immunoprecipitation experiments under a denaturing condition. Data before loading adjustment were used for quantification. (#$p < 0.05$ compared with wild-type [WT]-WNK4 without KLHL3; *$p < 0.05$ compared with WT-WNK4 with KLHL3; n = 3; mean ± SEM).

See also Figure S1.

Olympus, Tokyo) (Kuroki et al., 2007), in the presence of different concentrations of GST-KLHL3. As shown in Figure 4, the diffusion time of TAMRA-labeled peptide became slower as the concentration of GST-KLHL3 increased, indicating that the WNK4 peptide bound to GST- KLHL3. GST alone did not affect the diffusion time, and the introduction of a PHAII-causing mutation (D564A) abolished the decrease in diffusion time by GST-KLHL3, clearly indicating that KLHL3 directly binds to WNK4.

WNK4 Protein Level Increased in the PHAII Model Mouse (*Wnk4*$^{D561A/+}$) Kidney

To determine whether the mechanism clarified in the cell culture studies was in fact working in the in vivo kidney, we re-evaluated our PHAII model mice carrying the D561A WNK4 mutation, which is equivalent to the human D564A mutation.

By using a recently generated WNK4 antibody that recognizes the amino terminus of WNK4 (Ohno et al., 2011), we found that the WNK4 protein level was significantly increased in the *Wnk4*$^{D561A/+}$ mouse kidney (Figure 5A), which we missed in our initial report (Yang et al., 2007). The specificity of this WNK4 antibody was rigorously verified (Ohno et al., 2011) and also recently confirmed by using *WNK4* knockout mice (Figure S2). Furthermore, the *Wnk4*$^{D561A/D561A}$ homozygous mouse showed a more increased WNK4 protein level, suggesting that the mutation may have a substantial effect in the regulation of the WNK4 protein level in vivo. We confirmed that the WNK4 messenger RNA (mRNA) level was not increased in the *Wnk4*$^{D561A/D561A}$ homozygous mouse kidney (Figure 5B), indicating that the increase in the WNK4 protein level was not caused by transcriptional activation.

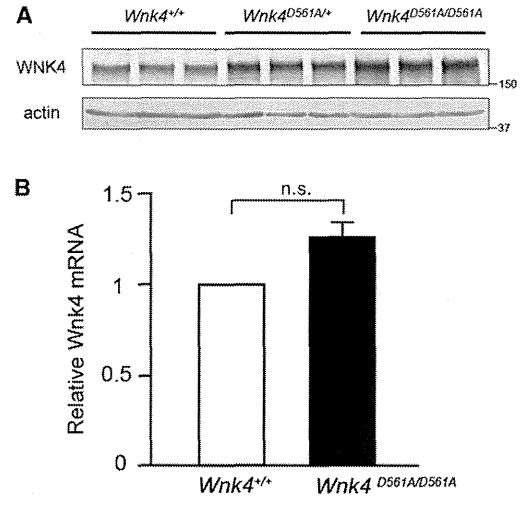

Figure 5. Increased WNK4 Protein Levels in *Wnk4*$^{D561A/+}$ and *Wnk4*$^{D561A/D561A}$ Knockin Mice

(A) WNK4 in *Wnk4*$^{D561A/+}$ and *Wnk4*$^{D561A/D561A}$ mice was increased 2.2 ± 0.1- and 2.7 ± 0.2-fold, respectively, compared with that in wild-type mice (n = 6, mean ± SEM).

(B) *WNK4* transcription was not increased in the *Wnk4*$^{D561A/D561A}$ PHAII model mouse. Quantitative RT-PCR revealed that WNK4 mRNA levels in *Wnk4*$^{+/+}$ (open bar) and *Wnk4*$^{D561A/D561A}$ (closed bar) mouse kidneys were not statistically different (mean ± SEM; n = 6; p = 0.34). n.s., not significant.

See also Figure S2.

Increased Expression of WNK4 in the Kidney Induced the Activation of the WNK-OSR1/SPAK-NCC Signal Cascade

To confirm whether the increased WNK4 protein level activates OSR1/SPAK-NCC signaling in the kidney, we generated bacterial artificial chromosome (BAC)-transgenic (TG) mice harboring multiple copies of the wild-type *WNK4* gene, as previously reported (Lalioti et al., 2006). As shown in Figure 6A, we presented the results of two representative transgenic lines; one had a low copy number of the transgene (two copies) and the other had a high copy number (thirty copies). WNK4 protein levels in the kidneys of low copy number (LC) and high copy number (HC) TG mice were increased 1.7 ± 0.1 (mean ± SEM)-fold in LC-TG mice and 9.1 ± 0.2-fold in HC-TG mice (n = 5), compared with those of wild-type mice. The phosphorylation of OSR1, SPAK, and NCC in the kidney (Figure 6A) clearly increased as the WNK4 protein levels increased in the TG mice. Immunofluorescence of phosphorylated NCC and WNK4 also clearly showed the overexpression of WNK4 and the increased phosphorylation of NCC in the distal convoluted tubules (Figure S3), confirming the activation of WNK-OSR1/SPAK-NCC signaling in the TG mice. Nighttime systolic, diastolic, and mean blood pressure and daytime diastolic blood pressure were significantly increased as the WNK4 protein levels increased in the TG mice (Figure 6B). The blood pressure in these TG mice was also comparable to that of *Wnk4*$^{D561A/+}$ knockin mice measured by the same telemetry system (wild-type versus *Wnk4*$^{D561A/+}$ knockin: 118.3 ± 0.77 versus 125.1 ± 0.90, mean ±SEM, n = 4, $p < 0.05$). The LC-TG and HC-TG mice also showed hyperkalemia and metabolic acidosis (Table 1) like *Wnk4*$^{D561A/+}$ knockin mice, and these phenotypes were more severe in HC-TG than LC-TG mice. We also investigated the phosphorylation status of NCC in two additional lines of transgene: one with no increase in WNK4 protein with two copies of the transgene, suggesting that the copy number of the transgene did not assure overexpression of the gene product, and the other with a robust increase in WNK4 protein with twenty copies of the transgene. The increased phosphorylation of NCC was only observed in the line with WNK4 overexpression (Figure S4). These results clearly indicate that the activation of the WNK-OSR1/SPAK-NCC cascade and the induction of PHAII phenotypes were dependent on the increased WNK4 protein levels in the in vivo kidney.

DISCUSSION

We previously demonstrated the activation of the WNK-OSR1/SPAK-NCC phosphorylation cascade in the mouse model of PHAII, *Wnk4*$^{D561A/+}$ knockin mice (Yang et al., 2007), by developing phosphospecific antibodies for residues of the amino-terminal domain of NCC (Chiga et al., 2008; Yang et al., 2007). Then, we and others clarified that this signal cascade was important in blood pressure regulation under certain pathophysiological conditions other than PHAII (Hoorn et al., 2011; Komers et al., 2012; San-Cristobal et al., 2009; Sohara et al., 2011). Thus, there is wide agreement (Gamba, 2012) that the

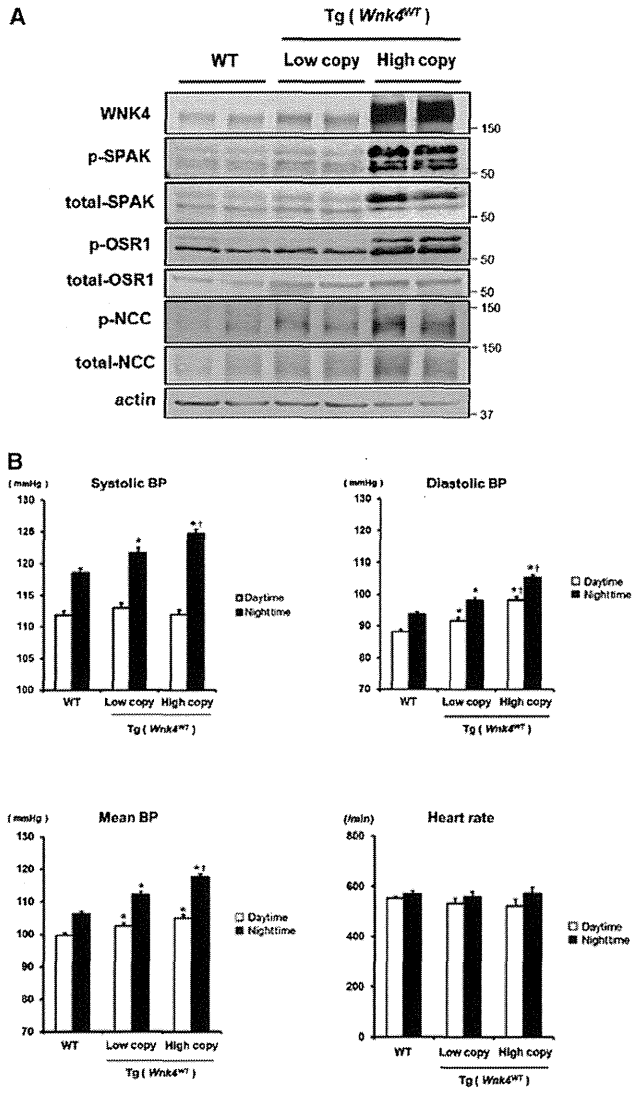

Figure 6. Generation and Analysis of *WNK4* TG Mice

(A) Status of the WNK-OSR1/SPAK-NCC phosphorylation cascade in the *WNK4* TG mice (Tg(*Wnk4*^{WT})). WNK4 protein levels in the kidneys of LC (two copies) and HC (thirty copies) TG mice were increased 1.7 ± 0.1- and 9.1 ± 0.2-fold, respectively (*p < 0.05, n = 5, mean ± SEM). NCC phosphorylation in these mice was significantly increased, compared with that of wild-type mice (p < 0.05, n = 5, mean ± SEM). The phosphorylation of SPAK in LC-TG and HC-TG mice and that of OSR1 in HC-TG mice was also significantly increased compared to that of wild-type mice (p < 0.05, n = 5, mean ± SEM). The total and phosphorylated OSR1, SPAK, and NCC in HC-TG mice were significantly increased compared with those in LC-TG mice (p < 0.05, n = 5, mean ± SEM). (B) Nighttime systolic, diastolic, and mean blood pressure (BP) and daytime diastolic blood pressure were significantly increased as the WNK4 protein levels increased in the Tg(*Wnk4*^{WT}) mice. Values were collected over 7 consecutive days (daytime: from 8:00 until 20:00; nighttime: from 20:00 until 8:00). *p < 0.05 versus WT; †p < 0.05 versus LC; WT n = 5; LC-TG n = 5; HC-TG n = 4; mean ± SEM.

See also Figures S3 and S4.

Table 1. Blood Biochemistries of WT and LC- and HC-Tg(*Wnk4*^{WT}) Mice

	WT Mice (n = 16)	LC (n = 16) Tg(*Wnk4*^{WT}) Mice	HC (n = 16) Tg(*Wnk4*^{WT}) Mice
Na (mmol/l)	145.4 ± 0.3	147.0 ± 0.3*	147.4 ± 0.5**
K (mmol/l)	4.2 ± 0.1	5.1 ± 0.1**	5.5 ± 0.1**,†
Cl (mmol/l)	110.3 ± 0.3	111.9 ± 0.3**	112.8 ± 0.5**
HCO_3^- (mmol/l)	24.4 ± 0.3	21.5 ± 0.4**	21.1 ± 0.3**
pH (venous)	7.302 ± 0.023	7.245 ± 0.003**	7.220 ± 0.004**,††

Values are the mean ± SEM. *, p < 0.05; **, p < 0.01 versus wild-type (WT) (one-way ANOVA followed by Tukey's post hoc test). †, p < 0.05; ††, p < 0.01 versus low copy number (one-way ANOVA followed by Tukey's test). Low copy number (LC) and high copy number (HC) Tg(*Wnk4*^{WT}) mice showed hyperkalemia and metabolic acidosis.

phosphorylation status of NCC governed by WNK-OSR1/SPAK signaling reflects NCC activity in vivo. Given that PHAII is a thiazide-sensitive disease, we speculated that *KLHL3* and *Cullin3* mutations would also activate the WNK-OSR1/SPAK-NCC phosphorylation cascade. Gamba's group also recently clarified that the major WNK kinase regulating NCC phosphorylation in the kidney is WNK4 (Castañeda-Bueno et al., 2012). Accordingly, we first performed coimmunoprecipitation assays of KLHL3 with the components of the WNK4-OSR1/SPAK-NCC cascade because KLHL proteins have been recently identified as substrate adaptors in the Cullin3-based ubiquitin E3 ligase (Cirak et al., 2010; Kigoshi et al., 2011; Lee et al., 2010; Lin et al., 2011).

We found that KLHL3 showed a clear interaction only with WNK4 among the components of the cascade. The direct binding of WNK4 to KLHL3 at the acidic motif was also confirmed in this study. In addition to the interaction, we showed that KLHL3 coexpression dramatically reduced both overexpressed and endogenous WNK4, indicating that KLHL3 is a strong regulator of WNK4 protein abundance within cells. Such an effect was reduced in the PHAII-causing mutations of WNK4 and KLHL3, resulting in a common consequence: the increase in WNK4 protein abundance. We also confirmed that the interaction of KLHL3 with WNK4 induced the ubiquitination of WNK4 in HEK293T cells and in in vitro ubiquitination assay. The reduced interaction of KLHL3 with WNK4 by PHAII-causing mutations in either protein also reduced the ubiquitination of WNK4, and the PHAII-causing mutant *Cullin3* was less able to reduce WNK4 protein abundance. Although we cannot exclude the possibility that KLHL3 may have targets other than WNK4, these results strongly suggest that WNK4 protein abundance within cells is regulated by KLHL3-Cullin3-mediated ubiquitination of WNK4 and that the major common molecular mechanism of PHAII is the impaired ubiquitination of WNK4.

Because the in vitro data could explain the molecular pathogenesis of PHAII caused by three different kinds of molecules, i.e., WNK4, KLHL3, and Cullin3, we verified this idea in vivo. Previously, WNK4 was shown to be able to phosphorylate and activate OSR1 and SPAK, as well as WNK1, in vitro (Moriguchi et al., 2005), and Ahlstrom and Yu (2009) reported in HEK293 cells that the intrinsic kinase activity of PHAII-causing mutant WNK4 was not different from that of wild-type WNK4. Given that the recent data on *WNK4* knockout mice (Castañeda-Bueno et al., 2012) clearly indicate that WNK4 is the major WNK kinase

Please cite this article in press as: Wakabayashi et al., Impaired KLHL3-Mediated Ubiquitination of WNK4 Causes Human Hypertension, Cell Reports (2013), http://dx.doi.org/10.1016/j.celrep.2013.02.024

in the kidney, we think it is reasonable to infer that the increased WNK4 abundance in the kidney, as we observed in the *Wnk4*$^{D561A/+}$ mice, could activate the cascade and was the cause of PHAII. To further prove this idea, we generated wild-type *WNK4*-TG mice as previously reported (Lalioti et al., 2006). We evaluated several lines of TG mice with different levels of WNK4 protein overexpression, and we think that *WNK4* TG mice could mimic *Wnk4*$^{D561A/+}$ knockin mice. We clearly showed that the WNK-OSR1/SPAK-NCC cascade and the PHAII phenotypes were induced according to the increases in wild-type WNK4 protein overexpression. This WNK4-dependent expression of phenotypes strongly suggests that these phenotypes were not caused by a nonspecific effect of the transgene. Several studies, mainly performed in *Xenopus* oocytes and in cultured cells, have shown that WNK4 behaves as a negative regulator of NCC (Wilson et al., 2003; Yang et al., 2003). This negative effect was shown to be a kinase-activity-independent function of WNK4 (Yang et al., 2005), suggesting that the kinase-activity-dependent positive and -activity-independent negative effects of WNK4 might act on NCC concomitantly and that the net effect might differ in different experimental situations. In fact, the *WNK4*-TG mouse with the wild-type *WNK4* gene generated by Lalioti et al. (2006) was reported to show Gitelman-syndrome-like phenotypes rather than those of PHAII, which is contrary to our TG data in this study. No data regarding the status of the WNK-OSR1/SPAK-NCC cascade and WNK4 protein level in their TG mice have been reported (Lalioti et al., 2006). In addition, it was not clear whether the negative effect of wild-type WNK4 on NCC was dependent on WNK4 protein levels, because only a single line of TG mice was reported. Therefore, the reason for the discrepancy between our *WNK4* TG study and Lalioti's study is not clear. It is possible that the level of WNK4 protein in their TG mice might be less than those in our *WNK4* TG mice and PHAII models (about 2-fold increases); they mentioned that only a 50% increase in WNK4 mRNA expression was observed in their TG mice. The net effect of WNK4 on NCC might be expressed as a negative effect under such conditions. Our previous study using the triple knockin mice of *WNK4*, *OSR1*, and *SPAK* suggested that the contribution of this negative effect of WNK4 on NCC might be minimal in the kidney, at least under PHAII conditions (Chiga et al., 2011). Our TG data in this study also clearly indicate that the increase in WNK4 protein at the PHAII level or higher brought about a positive net effect on NCC.

Because NCC phosphorylation in the kidney is highly dependent on WNK4 (Castañeda-Bueno et al., 2012; Oi et al., 2012; Susa et al., 2012), we focused on WNK4 in this study. However, WNK kinases other than WNK4 may also be regulated by the KLHL3-Cullin3 complex. The amino acid sequence of the KLHL3 binding site in WNK4 is highly conserved in other WNK kinases (Figure 4), and we could observe that WNK1 protein, as well as WNK4 protein, was decreased by overexpression and increased by knockdown of KLHL3 (Figure S5). In this respect, WNK1 as well as WNK4 may be increased in the kidneys of patients with PHAII carrying the *KLHL3* and *Cullin3* mutations, thereby contributing to the activation of OSR1/SPAK-NCC signaling and to more severe PHAII phenotypes via Cullin3 and KLHL3 than those via WNK1 and WNK4 (Boyden et al., 2012). Because the PHAII-causing mutations of *WNK1* are the large deletions of intron 1, which reportedly increases *WNK1* transcription (Wilson et al., 2001), the mechanism clarified in this study may not be directly related to the pathogenesis of PHAII by the *WNK1* mutations. However, we may consider PHAII as a disease caused by increased WNK kinase abundance either by the dysregulation of transcription or by the ubiquitination of WNK kinases.

In summary, our study identified that WNK4 is a substrate of KLHL3-Cullin3-mediated ubiquitination and that the impaired ubiquitination of WNK4 is a common mechanism of PHAII by *WNK4*, *KLHL3*, and *Cullin3* PHAII-causing mutations. Additional studies may be necessary to confirm this pathogenic mechanism in vivo by generating *KLHL3* and *Cullin3* knockin mice carrying PHAII mutations.

EXPERIMENTAL PROCEDURES

Plasmids

Expression plasmids for 3×FLAG-tagged human WNK4 and 3×FLAG-tagged D564A human WNK4 have been described previously (Yamauchi et al., 2004). E562K and Q565E mutations were also introduced by using a QuikChange Site-Directed Mutagenesis Kit (Stratagene). The complementary DNA (cDNA) encoding Halo-tagged human KLHL3 in pFN21A vector (HT-KLHL3) was purchased from Promega, and a disease-causing mutation (R528H) was introduced. Human Cullin3 cDNA was isolated by RT-PCR using human prostate mRNA as a template, and the cDNA was cloned into 3×FLAG-CMV10 vector (Sigma-Aldrich). T7-tagged OSR1, T7-tagged SPAK, and T7-tagged NCC expression plasmids in pRK5 vector were kindly provided by T. Moriguchi and H. Shibuya (Moriguchi et al., 2005). T7-tagged human WNK4 construct was also generated by introducing the T7 epitope by PCR. HA_4-tagged ubiquitin expression vector was kindly provided by T. Ohta (St. Marianna University School of Medicine).

Cell Culture and Transfections

HEK293T cells were cultured in Dulbecco's modified Eagle's medium supplemented with 10% (v/v) fetal bovine serum, 2 mM L-glutamine, 100 U/ml penicillin, and 0.1 mg/ml streptomycin at 37°C in a humidified 5% CO_2 incubator. The mpkDCT cell line kindly provided by A. Vandewalle was cultured in a defined medium as described previously (Duong Van Huyen et al., 2001). HEK293T cells and mpkDCT cells (3×10^5 cells per 6 cm dish) were transfected by the indicated amount of plasmid DNA with Lipofectamine 2000 reagent (Invitrogen). For each transfection, 4~8 μg of expression vectors were used, and the total amount of plasmid DNA was adjusted by adding empty vectors. In preliminary experiments, FLAG-tagged BAP (Figure 2A) was used for evaluating the transfection efficiency of transient expression of FLAG-tagged WNK4.

Immunoprecipitation

HEK293T cells transfected with the indicated amount of DNA were lysed in a buffer (50 mM Tris-HCl [pH 7.5], 150 mM NaCl, 1% Nonidet P-40, 1 mM sodium orthovanadate, 50 mM sodium fluoride, and protease inhibitor cocktail) for 30 min at 4°C. When the cells were transfected with the HA-ubiquitin expression plasmid, the cells were treated with 1 μM epoxomicin (specific and irreversible proteasome inhibitor; Peptide Institute, Osaka, Japan) for 3 hr before harvesting. After centrifugation at 12,000 × *g* for 15 min, the protein concentration of the supernatants was measured, and equal amounts of the supernatants were used for immunoprecipitation with anti-FLAG M2 beads (Sigma-Aldrich) or anti-T7 beads (Merck Millipore) for 2 hr at 4°C. Thereafter, the precipitants were washed with the lysis buffer and the immunoprecipitates were eluted in SDS sample buffer after boiling for 5 min. To detect ubiquitination of WNK4 in denatured samples, the cells transfected with various plasmids were lysed in 2% SDS buffer (2% SDS, 150 mM NaCl, 10 mM Tris-HCl

[pH 8.0], 2 mM sodium orthovanadate, 50 mM sodium fluoride, and 1× protease inhibitors) and boiled for 10 min, followed by sonication. Before immunoprecipitation, the lysates were diluted 1:10 in a dilution buffer (10 mM Tris-HCl [pH 8.0], 150 mM NaCl, 2 mM EDTA, and 1% Triton X-100), incubated at 4°C for 1 hr with rotation, and centrifuged at 12,000 × *g* for 15 min.

Immunoblotting

Whole homogenates of mouse kidney without the nuclear fraction (600 × *g*) or the crude membrane fraction (17,000 × *g*) were subjected to semiquantitative immunoblotting, as described previously (Yang et al., 2007). Cells transfected with the indicated amount of plasmid DNA were lysed in lysis buffer (50 mM Tris-HCl [pH 7.5], 150 mM NaCl, 1% Nonidet P-40, 1 mM sodium orthovanadate, 50 mM sodium fluoride, and protease inhibitor cocktail [Roche Diagnostics]) for 30 min at 4°C. After centrifugation at 12,000 × *g* for 15 min, the supernatants were boiled with SDS sample buffer (Cosmo Bio USA) and subjected to SDS-PAGE. Blots were probed with the following primary antibodies: anti-total NCC (Ohno et al., 2011), anti-phosphorylated NCC (pSer71) (Yang et al., 2007), anti-WNK4 (Ohno et al., 2011; Ohta et al., 2009), anti-total OSR1 (M9; Abnova), anti-phosphorylated OSR1 (Ohta et al., 2009), anti-total SPAK (Cell Signaling Technology), anti-phosphorylated SPAK (Yang et al., 2010), anti-GAPDH (Santa Cruz Biotechnology), anti-actin (Cytoskeleton), anti-HA (Merck Millipore), anti-KLHL3 (Abcam), anti-Cullin3 (Abcam), anti-FLAG (Sigma-Aldrich), anti-Halo (Promega), and anti-T7 (Merck Millipore). Specificities of anti-pNCC, pOSR1, and pSPAK were rigorously determined in our previous reports (Chiga et al., 2008; Ohta et al., 2009; Yang et al., 2007, 2010). Alkaline-phosphatase-conjugated immunoglobulin G antibodies (Promega) were used as secondary antibodies for immunoblotting. The intensity of the bands was analyzed and quantified by using ImageJ software (National Institutes of Health).

In Vitro Ubiquitination Assay

cDNA encoding human WNK4 (490–626) with a C-terminal His-tag was amplified by PCR and cloned into pGEX6p-1 vector. Recombinant GST fusion WNK4 protein was expressed in BL21 *E. coli* cells and purified by using glutathione sepharose beads. KLHL3-Cullin3 complexes were immunoprecipitated from the lysates of HEK293T cells transiently expressing FLAG-Cullin3 and Halo-KLHL3. Then, the complexes were incubated in 20 μl of reaction buffer (50 mM Tris-HCl [pH 7.4], 2.5 mM MgCl2, 0.5 mM DTT, and 2 mM ATP) for 2 hr at 30°C with purified GST-WNK4-His (5 μg), 100 ng recombinant human E1 (Boston Biochem), 500 ng recombinant human UbcH5a/UBE2D1 (Boston Biochem), and 2.5 μg recombinant human ubiquitin (Boston Biochem). The reaction was terminated by the addition of SDS-PAGE sample buffer, followed by boiling for 5 min. The reaction mixtures were then subjected to immunoblot analyses with ubiquitin (Cell Signaling Technology) or His (Abcam) antibodies.

Quantitative RT-PCR

Both kidneys were removed, immediately frozen in dry ice, and fragmented and homogenized in TRIzol Reagent (Invitrogen). Isolated total RNA was reverse-transcribed by using Omniscript reverse transcriptase (QIAGEN), and quantitative real-time PCR analysis was performed in triplicate by using SYBR Green I (Roche Applied Science) on LightCycler 2.0 (Roche). Amplification primers for *WNK4* were the same as reported previously (O'Reilly et al., 2006), and the primers for GAPDH were purchased from Roche Diagnostics. WNK4 mRNA levels were corrected by GAPDH mRNA levels.

Fluorescence Correlation Spectroscopy

Fluorescent TAMRA-labeled WNK4 peptides covering the PHAII mutation sites were prepared (Hokkaido System Science, Hokkaido, Japan). The sequence details of the peptides are shown in Figure 4. Human full-length KLHL3 was cloned into pGEX6P-1 vector. Recombinant GST fusion KLHL3 protein was expressed in BL21 *E. coli* cells and purified by using glutathione sepharose beads. The TAMRA-labeled WNK4 peptides were incubated at room temperature for 30 min with different concentrations of GST-KLHL3 (0–2 μM) in 1 × PBS with 0.05% Tween 20 reaction buffer, and the FCS measurements of single-molecule fluorescence were performed using the FluoroPoint-Light analytical system (Olympus) (Kuroki et al., 2007). The assay was performed in a 384-well plate. All experiments were performed in 10 s of data-acquisition time, and the measurements were repeated five times per sample.

Production of *Wnk4* BAC TG Mice

The BAC clone bMQ428o09, which contains the mouse genomic *Wnk4* locus, was used. For Southern blot analysis and PCR genotyping, a new *Spe*I site was created in intron 6 of the *Wnk4* genomic locus. The BAC modification was performed as previously described (Warming et al., 2005). Purified BAC DNA was then digested with *Swa*I, and the desired 36.8 kb fragment was isolated after fractionation via inverted pulse field gel electrophoresis, as reported previously (Lalioti et al., 2006). The purified fragment was injected into one-cell embryos of C57BL/6J mice. The copy number of the transgene was estimated by Southern blotting and quantitative PCR. The Animal Care and Use Committee of Tokyo Medical and Dental University approved this experiment (0120038B).

Blood Pressure Measurements

We measured blood pressure by using a radiotelemetric method (Mills et al., 2000) in which a blood pressure transducer (Data Sciences International, St. Paul, MN, USA) was inserted into the left carotid artery. Seven days after transplantation, each mouse was housed individually in a standard cage on a receiver under a 12 hr light-dark cycle. Systolic and diastolic blood pressure, heart rate, and activity were recorded every minute via radiotelemetry. Mice showed alternating periods of high activity (20:00–8:00) and low activity (8:00–20:00). For each mouse, we measured blood pressure values for more than 5 consecutive days and calculated the mean ± SEM of all values during both the high- and low-activity periods.

Blood Data Analyses

Blood for electrolyte analyses was obtained as described previously (Yang et al., 2007). Electrolyte levels were determined with an i-STAT analyzer (Fuso Pharmaceutical Industries, Osaka, Japan).

Statistical Analysis

Comparisons between the two groups were performed with unpaired t tests. ANOVA with Tukey's post hoc test was used to evaluate statistical significance in the comparison among multiple groups. p values <0.05 were considered statistically significant. Data are presented as the mean ± SEM.

SUPPLEMENTAL INFORMATION

Supplemental Information includes five figures and can be found with this article online at http://dx.doi.org/10.1016/j.celrep.2013.02.024.

LICENSING INFORMATION

ACKNOWLEDGMENTS

This study was supported in part by Grants-in-Aid for Scientific Research (A) from the Japan Society for the Promotion of Science; a Health and Labor Sciences Research Grant from the Ministry of Health, Labor, and Welfare; the Salt Science Research Foundation (grant no. 1026, 1228); the Takeda Science Foundation; and a Banyu Foundation Research Grant.

Received: November 28, 2012
Revised: January 25, 2013
Accepted: February 13, 2013
Published: February 28, 2013

Please cite this article in press as: Wakabayashi et al., Impaired KLHL3-Mediated Ubiquitination of WNK4 Causes Human Hypertension, Cell Reports (2013), http://dx.doi.org/10.1016/j.celrep.2013.02.024

REFERENCES

Achard, J.M., Disse-Nicodeme, S., Fiquet-Kempf, B., and Jeunemaitre, X. (2001). Phenotypic and genetic heterogeneity of familial hyperkalaemic hypertension (Gordon syndrome). Clin. Exp. Pharmacol. Physiol. *28*, 1048–1052.

Ahlstrom, R., and Yu, A.S. (2009). Characterization of the kinase activity of a WNK4 protein complex. Am. J. Physiol. Renal Physiol. *297*, F685–F692.

Bergaya, S., Faure, S., Baudrie, V., Rio, M., Escoubet, B., Bonnin, P., Henrion, D., Loirand, G., Achard, J.M., Jeunemaitre, X., and Hadchouel, J. (2011). WNK1 regulates vasoconstriction and blood pressure response to α 1-adrenergic stimulation in mice. Hypertension *58*, 439–445.

Boyden, L.M., Choi, M., Choate, K.A., Nelson-Williams, C.J., Farhi, A., Toka, H.R., Tikhonova, I.R., Bjornson, R., Mane, S.M., Colussi, G., et al. (2012). Mutations in kelch-like 3 and cullin 3 cause hypertension and electrolyte abnormalities. Nature *482*, 98–102.

Castañeda-Bueno, M., Cervantes-Pérez, L.G., Vázquez, N., Uribe, N., Kantesaria, S., Morla, L., Bobadilla, N.A., Doucet, A., Alessi, D.R., and Gamba, G. (2012). Activation of the renal Na+:Cl- cotransporter by angiotensin II is a WNK4-dependent process. Proc. Natl. Acad. Sci. USA *109*, 7929–7934.

Chiga, M., Rai, T., Yang, S.S., Ohta, A., Takizawa, T., Sasaki, S., and Uchida, S. (2008). Dietary salt regulates the phosphorylation of OSR1/SPAK kinases and the sodium chloride cotransporter through aldosterone. Kidney Int. *74*, 1403–1409.

Chiga, M., Rafiqi, F.H., Alessi, D.R., Sohara, E., Ohta, A., Rai, T., Sasaki, S., and Uchida, S. (2011). Phenotypes of pseudohypoaldosteronism type II caused by the WNK4 D561A missense mutation are dependent on the WNK-OSR1/SPAK kinase cascade. J. Cell Sci. *124*, 1391–1395.

Cirak, S., von Deimling, F., Sachdev, S., Errington, W.J., Herrmann, R., Bönnemann, C., Brockmann, K., Hinderlich, S., Lindner, T.H., Steinbrecher, A., et al. (2010). Kelch-like homologue 9 mutation is associated with an early onset autosomal dominant distal myopathy. Brain *133*, 2123–2135.

Duong Van Huyen, J.P., Bens, M., Teulon, J., and Vandewalle, A. (2001). Vasopressin-stimulated chloride transport in transimmortalized mouse cell lines derived from the distal convoluted tubule and cortical and inner medullary collecting ducts. Nephrol. Dial. Transplant. *16*, 238–245.

Gamba, G. (2012). Regulation of the renal Na+-Cl- cotransporter by phosphorylation and ubiquitylation. Am. J. Physiol. Renal Physiol. *303*, F1573–F1583.

Gordon, R.D. (1986). Syndrome of hypertension and hyperkalemia with normal glomerular filtration rate. Hypertension *8*, 93–102.

Hoorn, E.J., Walsh, S.B., McCormick, J.A., Fürstenberg, A., Yang, C.L., Roeschel, T., Paliege, A., Howie, A.J., Conley, J., Bachmann, S., et al. (2011). The calcineurin inhibitor tacrolimus activates the renal sodium chloride cotransporter to cause hypertension. Nat. Med. *17*, 1304–1309.

Kigoshi, Y., Tsuruta, F., and Chiba, T. (2011). Ubiquitin ligase activity of Cul3-KLHL7 protein is attenuated by autosomal dominant retinitis pigmentosa causative mutation. J. Biol. Chem. *286*, 33613–33621.

Komers, R., Rogers, S., Oyama, T.T., Xu, B., Yang, C.L., McCormick, J., and Ellison, D.H. (2012). Enhanced phosphorylation of Na(+)-Cl- co-transporter in experimental metabolic syndrome: role of insulin. Clin. Sci. *123*, 635–647.

Kuroki, K., Kobayashi, S., Shiroishi, M., Kajikawa, M., Okamoto, N., Kohda, D., and Maenaka, K. (2007). Detection of weak ligand interactions of leukocyte Ig-like receptor B1 by fluorescence correlation spectroscopy. J. Immunol. Methods *320*, 172–176.

Lalioti, M.D., Zhang, J., Volkman, H.M., Kahle, K.T., Hoffmann, K.E., Toka, H.R., Nelson-Williams, C., Ellison, D.H., Flavell, R., Booth, C.J., et al. (2006). Wnk4 controls blood pressure and potassium homeostasis via regulation of mass and activity of the distal convoluted tubule. Nat. Genet. *38*, 1124–1132.

Lee, Y.R., Yuan, W.C., Ho, H.C., Chen, C.H., Shih, H.M., and Chen, R.H. (2010). The Cullin 3 substrate adaptor KLHL20 mediates DAPK ubiquitination to control interferon responses. EMBO J. *29*, 1748–1761.

Lin, M.Y., Lin, Y.M., Kao, T.C., Chuang, H.H., and Chen, R.H. (2011). PDZ-RhoGEF ubiquitination by Cullin3-KLHL20 controls neurotrophin-induced neurite outgrowth. J. Cell Biol. *193*, 985–994.

Liu, Z., Xie, J., Wu, T., Truong, T., Auchus, R.J., and Huang, C.L. (2011). Down-regulation of NCC and NKCC2 cotransporters by kidney-specific WNK1 revealed by gene disruption and transgenic mouse models. Hum. Mol. Genet. *20*, 855–866.

Louis-Dit-Picard, H., Barc, J., Trujillano, D., Miserey-Lenkei, S., Bouatia-Naji, N., Pylypenko, O., Beaurain, G., Bonnefond, A., Sand, O., Simian, C., et al.; International Consortium for Blood Pressure (ICBP). (2012). KLHL3 mutations cause familial hyperkalemic hypertension by impairing ion transport in the distal nephron. Nat. Genet. *44*, 456–460, S1–S3.

McCormick, J.A., and Ellison, D.H. (2011). The WNKs: atypical protein kinases with pleiotropic actions. Physiol. Rev. *91*, 177–219.

McEvoy, J.D., Kossatz, U., Malek, N., and Singer, J.D. (2007). Constitutive turnover of cyclin E by Cul3 maintains quiescence. Mol. Cell. Biol. *27*, 3651–3666.

Mills, P.A., Huetteman, D.A., Brockway, B.P., Zwiers, L.M., Gelsema, A.J., Schwartz, R.S., and Kramer, K. (2000). A new method for measurement of blood pressure, heart rate, and activity in the mouse by radiotelemetry. J. Appl. Physiol. *88*, 1537–1544.

Moriguchi, T., Urushiyama, S., Hisamoto, N., Iemura, S., Uchida, S., Natsume, T., Matsumoto, K., and Shibuya, H. (2005). WNK1 regulates phosphorylation of cation-chloride-coupled cotransporters via the STE20-related kinases, SPAK and OSR1. J. Biol. Chem. *280*, 42685–42693.

O'Reilly, M., Marshall, E., Macgillivray, T., Mittal, M., Xue, W., Kenyon, C.J., and Brown, R.W. (2006). Dietary electrolyte-driven responses in the renal WNK kinase pathway in vivo. J. Am. Soc. Nephrol. *17*, 2402–2413.

Ohno, M., Uchida, K., Ohashi, T., Nitta, K., Ohta, A., Chiga, M., Sasaki, S., and Uchida, S. (2011). Immunolocalization of WNK4 in mouse kidney. Histochem. Cell Biol. *136*, 25–35.

Ohta, A., Rai, T., Yui, N., Chiga, M., Yang, S.S., Lin, S.H., Sohara, E., Sasaki, S., and Uchida, S. (2009). Targeted disruption of the Wnk4 gene decreases phosphorylation of Na-Cl cotransporter, increases Na excretion and lowers blood pressure. Hum. Mol. Genet. *18*, 3978–3986.

Oi, K., Sohara, E., Rai, T., Misawa, M., Chiga, M., Alessi, D.R., Sasaki, S., and Uchida, S. (2012). A minor role of WNK3 in regulating phosphorylation of renal NKCC2 and NCC co-transporters in vivo. Biol. Open *1*, 120–127.

Rossier, B.C., and Schild, L. (2008). Epithelial sodium channel: mendelian versus essential hypertension. Hypertension *52*, 595–600.

San-Cristobal, P., Pacheco-Alvarez, D., Richardson, C., Ring, A.M., Vazquez, N., Rafiqi, F.H., Chari, D., Kahle, K.T., Leng, Q., Bobadilla, N.A., et al. (2009). Angiotensin II signaling increases activity of the renal Na-Cl cotransporter through a WNK4-SPAK-dependent pathway. Proc. Natl. Acad. Sci. USA *106*, 4384–4389.

Shimkets, R.A., Warnock, D.G., Bositis, C.M., Nelson-Williams, C., Hansson, J.H., Schambelan, M., Gill, J.R., Jr., Ulick, S., Milora, R.V., Findling, J.W., et al. (1994). Liddle's syndrome: heritable human hypertension caused by mutations in the beta subunit of the epithelial sodium channel. Cell *79*, 407–414.

Sohara, E., Rai, T., Yang, S.S., Ohta, A., Naito, S., Chiga, M., Nomura, N., Lin, S.H., Vandewalle, A., Ohta, E., et al. (2011). Acute insulin stimulation induces phosphorylation of the Na-Cl cotransporter in cultured distal mpkDCT cells and mouse kidney. PLoS ONE *6*, e24277.

Susa, K., Kita, S., Iwamoto, T., Yang, S.S., Lin, S.H., Ohta, A., Sohara, E., Rai, T., Sasaki, S., Alessi, D.R., and Uchida, S. (2012). Effect of heterozygous deletion of WNK1 on the WNK-OSR1/ SPAK-NCC/NKCC1/NKCC2 signal cascade in the kidney and blood vessels. Clin. Exp. Nephrol. *16*, 530–538.

Warming, S., Costantino, N., Court, D.L., Jenkins, N.A., and Copeland, N.G. (2005). Simple and highly efficient BAC recombineering using galK selection. Nucleic Acids Res. *33*, e36.

Wilson, F.H., Disse-Nicodème, S., Choate, K.A., Ishikawa, K., Nelson-Williams, C., Desitter, I., Gunel, M., Milford, D.V., Lipkin, G.W., Achard, J.M., et al. (2001). Human hypertension caused by mutations in WNK kinases. Science *293*, 1107–1112.

Wilson, F.H., Kahle, K.T., Sabath, E., Lalioti, M.D., Rapson, A.K., Hoover, R.S., Hebert, S.C., Gamba, G., and Lifton, R.P. (2003). Molecular pathogenesis of inherited hypertension with hyperkalemia: the Na-Cl cotransporter is inhibited by wild-type but not mutant WNK4. Proc. Natl. Acad. Sci. USA *100*, 680–684.

Yamauchi, K., Rai, T., Kobayashi, K., Sohara, E., Suzuki, T., Itoh, T., Suda, S., Hayama, A., Sasaki, S., and Uchida, S. (2004). Disease-causing mutant WNK4 increases paracellular chloride permeability and phosphorylates claudins. Proc. Natl. Acad. Sci. USA *101*, 4690–4694.

Yang, C.L., Angell, J., Mitchell, R., and Ellison, D.H. (2003). WNK kinases regulate thiazide-sensitive Na-Cl cotransport. J. Clin. Invest. *111*, 1039–1045.

Yang, C.L., Zhu, X., Wang, Z., Subramanya, A.R., and Ellison, D.H. (2005). Mechanisms of WNK1 and WNK4 interaction in the regulation of thiazide-sensitive NaCl cotransport. J. Clin. Invest. *115*, 1379–1387.

Yang, S.S., Morimoto, T., Rai, T., Chiga, M., Sohara, E., Ohno, M., Uchida, K., Lin, S.H., Moriguchi, T., Shibuya, H., et al. (2007). Molecular pathogenesis of pseudohypoaldosteronism type II: generation and analysis of a Wnk4(D561A/+) knockin mouse model. Cell Metab. *5*, 331–344.

Yang, S.S., Lo, Y.F., Wu, C.C., Lin, S.W., Yeh, C.J., Chu, P., Sytwu, H.K., Uchida, S., Sasaki, S., and Lin, S.H. (2010). SPAK-knockout mice manifest Gitelman syndrome and impaired vasoconstriction. J. Am. Soc. Nephrol. *21*, 1868–1877.

GATA-2 *anomaly and clinical phenotype of a sporadic case of lymphedema, dendritic cell, monocyte, B- and NK-cell (DCML) deficiency, and myelodysplasia*

Hiroyuki Ishida, Kosuke Imai, Kenichi Honma, Shin-ichi Tamura, Toshihiko Imamura, Masafumi Ito & Shigeaki Nonoyama

European Journal of Pediatrics

ISSN 0340-6199

Eur J Pediatr
DOI 10.1007/s00431-012-1715-7

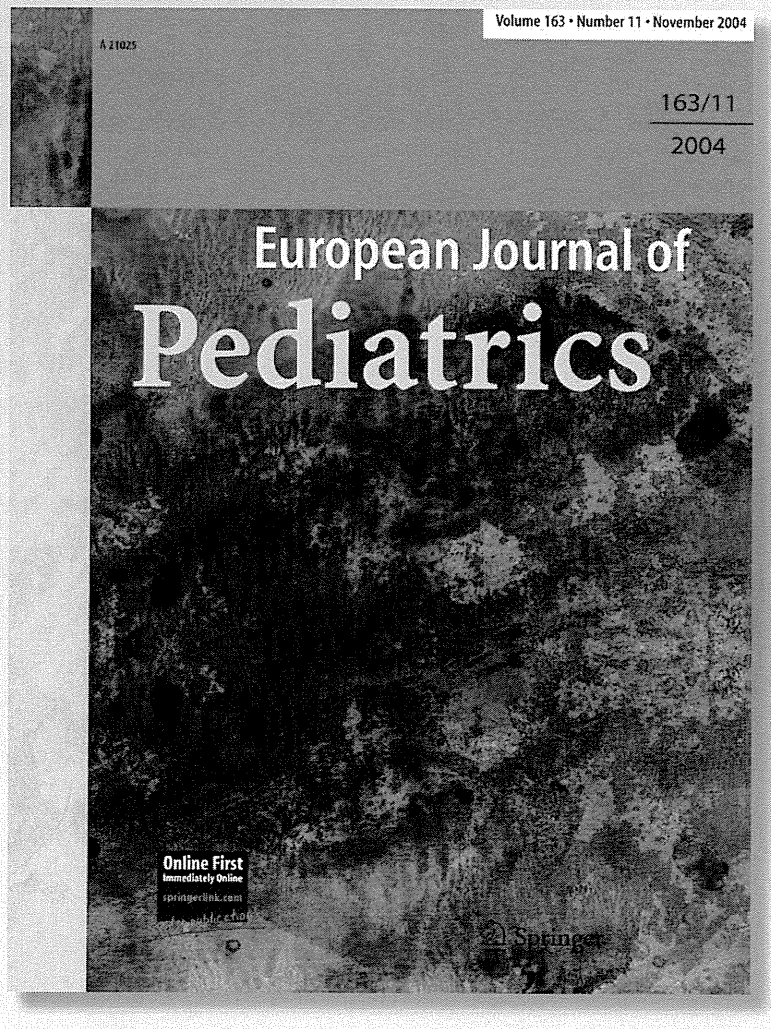

Springer

Eur J Pediatr
DOI 10.1007/s00431-012-1715-7

CASE REPORT

GATA-2 anomaly and clinical phenotype of a sporadic case of lymphedema, dendritic cell, monocyte, B- and NK-cell (DCML) deficiency, and myelodysplasia

Hiroyuki Ishida · Kosuke Imai · Kenichi Honma · Shin-ichi Tamura · Toshihiko Imamura · Masafumi Ito · Shigeaki Nonoyama

Received: 14 December 2011 / Accepted: 29 February 2012

Abstract A Japanese patient presented with lymphedema, severe *Varicella zoster*, and *Salmonella* infection, recurrent respiratory infections, panniculitis, monocytopenia, B- and NK-cell lymphopenia, and myelodysplasia. The phenotype was a mixture of the monocytopenia and mycobacterial infection (MonoMAC) and Emberger syndromes. Sequencing of the *GATA-2* cDNA revealed the heterozygous missense mutation 1187 G>A. This mutation resulted in the amino acid mutation Arg396Gln in the zinc fingers-2 domain, which is predicted to cause significant structural change and prevent a critical interaction with DNA. Functional analysis of the patient's *GATA-2* mutation is required to understand the relationship between these distinctive syndromes.

Keywords Emberger syndrome · MonoMAC · Monocytopenia · B- and NK-cell lymphopenia · Immunodeficiency · Myelodysplasia

H. Ishida (✉) · S.-i. Tamura
Department of Pediatrics and Blood and Marrow transplantation,
Matsushita Memorial Hospital,
5-55, Sotojima-cho,
Moriguchi 570-8540, Japan
e-mail: ishida.hiroyuki002@jp.panasonic.com

H. Ishida
e-mail: ishidah@koto.kpu-m.ac.jp

K. Imai
Department of Pediatrics, Tokyo Medical and Dental University,
5-45 Yushima 1-Chome,
Bunkyo-Ku, Tokyo 113-8510, Japan

K. Honma · S. Nonoyama
Department of Pediatrics, National Defense Medical College,
3-2 Namiki,
Tokorozawa 359-8513, Japan

T. Imamura
Department of Pediatrics,
Kyoto Prefectural University of Medicine,
465 Kajii-Cho, Kawaramachi-Hirokoji,
Kamigyo-Ku, Kyoto 602-8566, Japan

M. Ito
Department of Pathology,
Japanese Red Cross Nagoya First Hospital,
3-35 Michishita-cho, Nakamura-ku,
Nagoya 453-0046, Japan

Recent studies have characterized a novel primary immunodeficiency known as monocytopenia and mycobacterial infection (MonoMAC), also known as dendritic cell, monocyte, B and NK lymphoid (DCML) deficiency. This form of immunodeficiency occurs either as an autosomal dominant form or sporadically. It is primarily characterized by persistent and profound peripheral monocytopenia, diagnostic B- and NK-cell lymphocytopenia, and variable T cell lymphocytopenia, along with increased susceptibility to mycobacterium or papilloma virus infections [1, 2, 13]. Moreover, most patients with MonoMAC eventually develop acute myelogenous leukemia (AML) following myelodysplastic syndrome (MDS). Another rare disorder called Emberger syndrome (MIM614038) is characterized by congenital deafness and primary lymphedema of the lateral lower limb; typically, onset occurs in childhood and is associated with a predisposition to MDS or AML in addition to other minor anomalies such as hypotelorism and long tapering fingers. It is also a sporadic or familial disorder [8]. Familial MDS/AML without other hematopoietic defects has also been reported [6]. Surprisingly, it was reported recently that these three distinctive syndromes are all caused by *GATA-2*

Published online: 21 March 2012

mutations, which suggests that these syndromes are different phenotypes caused by the same genetic alteration [5–7, 9]. Here, we report the case of a patient with a *GATA-2* mutation bearing the characteristic features of MonoMAC/Emberger syndrome.

Case report

The patient was the second child of non-consanguineous parents. Neither the parents nor the elder brother had a history of increased susceptibility to infection. The medical history of the patient included BCG vaccination 3 months after birth without any side effects and a severe *Varicella zoster* infection at 2 years of age. After that, she suffered repeated upper and lower respiratory tract infections that required antibiotics. At 4 years of age, the patient's peripheral blood showed mild neutropenia and profound monocytopenia ($0–20\times10^6$/L), and mild hypocellularity but no dysplasia was observed in the bone marrow. At 8 years of age, she experienced a prolonged *Salmonella* enterocolitis infection. Lymphedema in the left leg first appeared at 13 years of age. She subsequently developed recurrent panniculitis. Recently, the patient (now 19 years old) was admitted to hospital with fever (with no apparent cause) and panniculitis (Fig. 1a). She had mild hypotelorism and lymphedema, with warts on her left leg (Fig. 1b). Her mental ability was appropriate for her age. An immunodeficiency was first suspected after the severe *Varicella zoster* and *Salmonella* infections during early childhood. The most recent recurrent episode of fever supported this suspicion.

Peripheral blood analysis revealed a white blood cell count of 1.5×10^9/L with 45% neutrophils, 54 % lymphocytes, and 1 % monocytes, a hemoglobin level of 11.0 g/dl, and a platelet count of 146×10^9/L. Flow cytometric analysis of the peripheral blood also revealed a deficiency in dendritic cells (lineage$^-$/DR$^+$/CD123$^+$ or CD11c$^+$ cells, 0%), B cells (CD19$^+$ cells, 0.7%), and NK cells (CD3$^-$/CD56$^+$ cells, 0.5%), and profound monocytopenia (CD14$^+$ cells, 0.2%). Lymphocytes comprised 97% T cells (CD4/8 ratio, 0.54), 33% of which were TCR $\gamma\delta^+$ T cells. Immunological analyses revealed IgG, IgA, IgM, and IgE levels of 711, 65, 131,

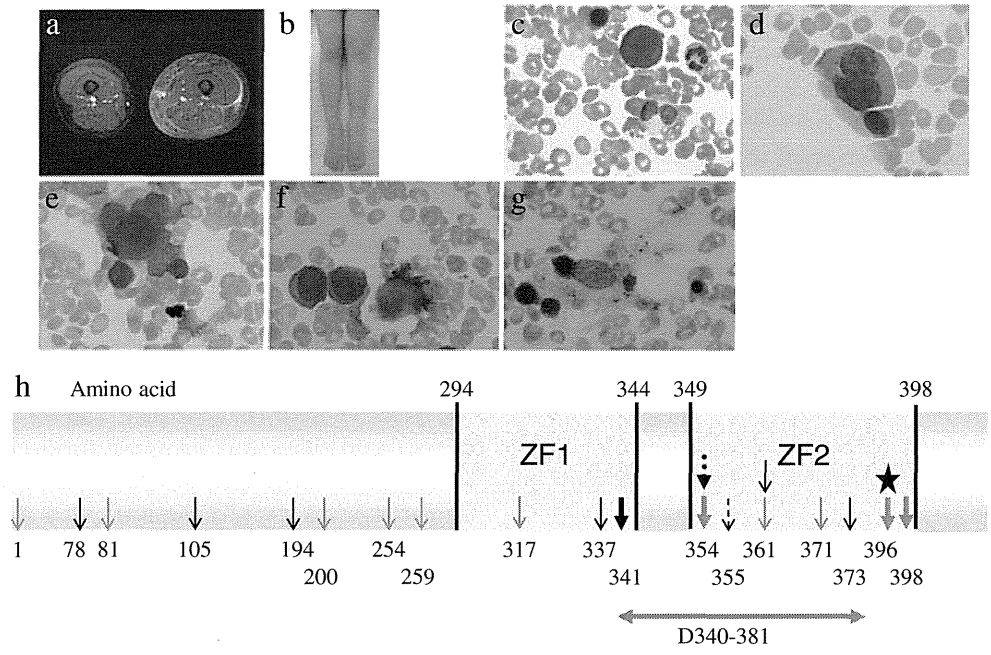

Fig. 1 Clinical and bone marrow features and *GATA-2* protein mutation sites. **a** A gadolinium-enhanced T2-weighted MRI image of the left thigh was performed when the patient developed panniculitis at 19 years of age. An increased signal was observed in the subcutaneous tissue and fascial layers. **b** After she was cured, the patient showed lymphedema in her left leg. **c–g** Bone marrow taken at the same time revealed decreased granule numbers within neutrophils and a pseudo-Pelger anomaly (**c**), binucleation (**d**), and megaloblastic changes in erythroblasts, dysplastic nuclei in megakaryocytes (**e**) and micromegakaryocytes (**f**), and hemophagocytosis (**g**). **h** Depiction of the *GATA-2* protein mutations previously identified in MonoMAC/DCML deficiency and Emberger syndrome. ZF1 and ZF2 are functional DNA-binding domains. The *star* indicates the Arg396Gln mutation identified in the present case. *Arrows* indicate previously reported mutations. These include missense, nonsense, and frameshift mutations (*short downward arrows*, respectively) and long deletions (*horizontal arrows*). *Black arrows* denote mutations associated with Emberger syndrome, *gray arrows* denote mutations associated with MonoMAC syndrome/DCML deficiency, *long horizontal arrows* indicate long deletions that have been observed in MonoMAC syndrome/DCML deficiency, *broken black arrows* denote mutations associated with familial MDS/AML, and *bold arrows* denote multiple pedigrees with the same mutation

and 5 mg/dl, respectively, and lymphocyte stimulation responses to phytohemagglutinin at the lower limits of the normal range. Antibody memory responses to infections contracted in early childhood (*Varicella* and *measles*) were maintained, and fibroblast sensitivity to radiation was normal. Flow FISH analysis of peripheral blood lymphocytes revealed normal telomere length; however, the peripheral blood contained 160 copies/μg WT1-mRNA (the upper limit of normal is 50 copies/μg RNA), and bone marrow aspirates showed hypocellularity, particularly of myeloid and lymphoid cells. Strikingly, despite monocytopenia in the peripheral blood, $CD64^+$ macrophages (accompanied by a few hemophagocytes) were observed in bone marrow specimens. Significant trilineage dysplasia was also present (Fig. 1c–g). Cytogenetic and chromosomal breakage analyses showed normal results. Meanwhile, profiles of familial peripheral blood showed a white blood cell count of 5.6×10^9/L with 50% neutrophils, 30% lymphocytes, and 8% monocytes, a hemoglobin level of 15.1 g/dl, and a platelet count of 199×10^9/L in the father; 5.1×10^9/L with 51 % neutrophils, 36% lymphocytes, and 9% monocytes, 10.7 g/dl, and 225×10^9/L in the mother; and 6.6×10^9/L with 41% neutrophils, 45% lymphocytes, and 10% monocytes, 15.4 g/dl, and 208×10^9/L in the brother. Flow cytometric analysis of peripheral blood samples taken from these family members showed a normal frequency of B cells ($CD19^+$ cells) and NK cells ($CD3^-/CD56^+$ cells) (the father 11 and 8%, the mother 10 and 12%, and the brother 9 and 15%, respectively). Taken together, these findings suggested that the patient might have sporadic MonoMAC/Emberger syndrome.

Sequencing of *GATA-2* cDNA revealed a 1187 G>A heterozygous missense mutation. This mutation resulted in an Arg396Gln substitution in the zinc finger-2 domain, which is predicted to cause significant structural changes that prevent critical interactions with DNA (Fig. 1h). Furthermore, sequencing of cDNA from her healthy familial members revealed no mutations, including 1187 G>A in *GATA-2* gene. Ultimately, the patient was diagnosed with MonoMAC/Emberger syndrome with a de novo *GATA-2* mutation.

Discussion

GATA-2 plays a critical role in both hematopoietic stem cell development and the maintenance of normal adult stem cell homeostasis [10]. It is likely that the significant protein structural alterations caused by mutations in *GATA-2* result in loss-of-function or have a dominant-negative effect on the DNA-binding ability of wild-type *GATA-2* [9] It seems reasonable to suggest that the loss of hematopoiesis-indispensable transcription factor activity results in impaired hematopoietic-cell differentiation and hematopoietic stem cell exhaustion; this in turn may promote the development of related diseases such as MDS and AML. Additional genetic alterations may also be required.

The patient's phenotype included hypotelorism, primary lymphedema (which had an onset during childhood before the recurrent episodes of panniculitis), peripheral monocytopenia, B- and NK-cell lymphocytopenia, neutropenia since early childhood, and myelodysplasia. The Arg396Glu mutation in *GATA-2* identified in this patient was not detected in 150 healthy individuals [7]. Taken together, these factors confirmed the diagnosis of MonoMAC/Emberger syndrome with a de novo *GATA-2* mutation; however, the *GATA-2* mutations alone cannot explain the phenotypic diversity between these three syndromes (MonoMAC, Emberger syndrome, and familial MDS/AML) and the presented patient. Interestingly, she developed neither BCG dissemination nor severe lymphadenitis after her BCG

Table 1 Summary of the clinical features of MonoMAC, Emberger syndrome, and the present case

	MonoMAC/DCML deficiency	Emberger syndrome	Present case
DCML[a] deficiency	+	+/–	+
MDS/AML	+	+	+
Lymphedema	ND	+	+
Deafness	ND	+/–	–
Hypotelorism	ND	+/–	+
Long slender fingers	ND	+/–	–
Mycobacterial infection	+	ND	–
Fungal infection	+/–	+/–	–
Papillomaviral infection/warts	+	+	+
Severe *varicella* and/or *Salmonella* infection	+/–	ND	+
Pulmonary alveolar proteinosis	+/–	ND	–
Panniculitis/erythema nodusa	+/–	+/–	+

ND not described, *MDS* myelodysplastic, *AML* acute myelogenous syndrome, + most cases, +/– some cases

[a]Dendritic cell, monocyte, B and NK lymphoid syndrome

vaccination 3 months after birth. This indicates normal functioning of tissue macrophages, because protective immunity to mycobacteria is dependent upon the interleukin (IL)-12/IL-23-interferon (IFN)-γ axis, possibly mediated by intracellular killing of phagocytes following the production of IFN-γ by CD4 T lymphocytes in response to IL-12/IL-23 secreted by infected macrophages [3]. Patients with MonoMAC/DCML deficiency show very low numbers of circulating monocytes and no detectable myeloid or plasmacytoid dendritic cells in the peripheral blood, but relatively normal numbers of Langerhans cells and tissue macrophages accompanied by prominent hemophagocytosis in the bone marrow [1, 2]. This supports the idea that tissue and marrow macrophages, in addition to Langerhans cells, may be maintained by a distinct precursor from circulating monocytes or dendritic cells [1].

Mansour et al. [8] reported that the age of onset of MDS/AML in Emberger syndrome is 9–14 (median 11) years of age. This appears to be earlier than that of MDS/AML in MonoMAC syndrome (7–52 years, median 32 years) [2]. Moreover, the level of WT1-mRNA in the peripheral blood increases significantly as MDS progresses and is a strong predictor of rapid AML transformation in adult patients with de novo MDS [11]. The level of WT1-mRNA in the peripheral blood of the current patient was as high as that in patients that show worse survival than those with a low level WT1 mRNA (10^2–10^4 vs. $<10^2$ copies/μg) [12]. However, it is unclear whether phenotypic variation and increased WT1 mRNA level are related to hematological disease progression. In any case, neutropenic patients who suffer recurrent infections and/or MDS are likely to need a transplant in the near future. Therefore, for such cases, we perform hematopoietic stem cell transplantation with a reduced intensity conditioning regimen before the disease has progressed [4]. Table 1 summarizes the clinical features of MonoMAC, Emberger syndrome, and the present case.

Our observations suggest that children with recurrent or prolonged common infections that respond to antibiotics and recover well may suffer from unknown primary immunodeficiencies. Although the relationship between *GATA-2* and lymphedema or deafness requires further investigation, tissue-specific lesions such as lymphedema provide important clues to primary immunodeficiencies that also affect non-hematopoietic cells.

Acknowledgments We are grateful to Dr. Sayoko Doisaki in the Department of Pediatrics, Nagoya University of Medical School, for the flow FISH analysis.

Conflict of Interest Statement The authors declare no competing financial interests.

References

1. Bigley V, Haniffa M, Doulatov S, Wang XN, Dickinson R, McGovernet N et al (2011) The human syndrome of dendritic cell, monocyte, B and NK lymphoid deficiency. J Exp Med 208:227–234
2. Calvo KR, Vinh DC, Maric I, Wang W, Noel P, Stetler-Stevenson M, Holland SM et al (2011) Myelodysplasia in autosomal dominant and sporadic monocytopenia immunodeficiency syndrome: diagnostic features and clinical implications. Haematologica 96:1221–1225
3. Carneiro-Sampaio M, Coutinho A (2007) Immunity to microbes: lessons from primary immunodeficiencies. Infect Immun 75:1545–1555
4. Cuellar-Rodriguez J, Gea-Banacloche J, Freeman AF, Hsu AP, Zerbe CS, Calvo KR et al (2011) Successful allogeneic hematopoietic stem cell transplantation for GATA2 deficiency. Blood 118:3715–3720
5. Dickinson RE, Griffin H, Bigley V, Reynard LN, Hussain R, Haniffa M et al (2011) Exome sequencing identifies *GATA-2* mutation as the cause of dendritic cell, monocyte, B and NK lymphoid deficiency. Blood 118:2656–2658
6. Hahn CN, Chong CE, Carmichael CL, Wilkins EJ, Brautigan PJ, Li XC et al (2011) Heritable GATA2 mutations associated with familial myelodysplastic syndrome and acute myeloid leukemia. Nat Genet 43:1012–1017
7. Hsu AP, Sampaio EP, Khan J, Calvo KR, Lemieux JE, Patel SY et al (2011) Mutations in GATA2 are associated with the autosomal dominant and sporadic monocytopenia and mycobacterial infection (MonoMAC) syndrome. Blood 118:2653–2655
8. Mansour S, Connell F, Steward C, Ostergaard P, Brice G, Smithson S et al (2010) Lymphoedema research consortium. Emberger syndrome-primary lymphedema with myelodysplasia: report of seven new cases. Am J Med Genet A 152A:2287–2296
9. Ostergaard P, Simpson MA, Connell FC, Steward CG, Brice G, Woollard WJ et al (2011) Mutations in GATA2 cause primary lymphedema associated with a predisposition to acute myeloid leukemia (Emberger syndrome). Nat Genet 43:929–931
10. Rodrigues NP, Boyd AS, Fugazza C, May GE, Guo Y, Tipping AJ et al (2008) *GATA-2* regulates granulocyte-macrophage progenitor cell function. Blood 112:4862–4873
11. Tamaki H, Ogawa H, Ohyashiki K, Ohyashiki JH, Iwama H, Inoue K et al (1999) The Wilms' tumor gene WT1 is a good marker for diagnosis of disease progression of myelodysplastic syndromes. Leukemia 13:393–399
12. Tamura H, Dan K, Yokose N, Iwakiri R, Ohta M, Sakamaki H et al (2010) Prognostic significance of WT1 mRNA and anti-WT1 antibody levels in peripheral blood in patients with myelodysplastic syndromes. Leuk Res 34:986–990
13. Vinh DC, Patel SY, Gl U, Anderson VL, Freeman AF, Olivier KN et al (2010) Autosomal dominant and sporadic monocytopenia with susceptibility to mycobacteria, fungi, papillomaviruses, and myelodysplasia. Blood 115:1519–1529

Clinical Endocrinology (2012) 77, 628–634 doi: 10.1111/j.1365-2265.2012.04390.x

ORIGINAL ARTICLE

Endocrine complications in primary immunodeficiency diseases in Japan

Takafumi Nozaki*, Hidetoshi Takada*, Masataka Ishimura*, Kenji Ihara*, Kohsuke Imai†, Tomohiro Morio†, Masao Kobayashi‡, Shigeaki Nonoyama§ and Toshiro Hara*

*Department of Pediatrics, Graduate School of Medical Sciences, Kyushu University, Fukuoka, †Department of Pediatrics and Developmental Biology, Graduate School of Medical and Dental Sciences, Tokyo Medical and Dental University, Tokyo, ‡Department of Pediatrics, Graduate School of Biomedical Sciences, Hiroshima University, Hiroshima, and §Department of Pediatrics, National Defense Medical College, Tokorozawa, Japan

Summary

Background In spite of the accumulating evidence on the interaction between the immune and endocrine systems based on the recent progress in molecular genetics, there have been few epidemiological studies focused on the endocrine complications associated with primary immunodeficiency diseases (PID).

Objective To investigate the prevalence and clinical features of endocrine complications in patients with PID in a large-scale study.

Design and participants This survey was conducted on patients with PID who were alive on 1 December 2008 and those who were newly diagnosed and died between 1 December 2007 and 30 November 2008 in Japan. We investigated the prevalence and the clinical data of the endocrine complications in 923 patients with PID registered in the secondary survey.

Results Among 923 PID patients, 49 (5·3%) had endocrine disorders. The prevalence of the endocrine diseases was much higher in patients with PID than in the general population in the young age group, even after excluding patients with immune dysregulation.

Conclusions Endocrine disorders are important complications of PID. Analysis of the endocrine manifestations in patients with PID in a large-scale study may provide further insights into the relationship between the immune and endocrine systems.

(Received 15 November 2011; returned for revision 23 December 2011; finally revised 19 January 2012; accepted 13 March 2012)

Introduction

A wide variety of clinical complications have been described in primary immunodeficiency diseases (PID).[1,2] PID have been reported to be associated with an increased risk of cancer, in particular non-Hodgkin lymphoma,[2] and the contribution of immune dysfunction in PID to cancer risk is receiving much attention. It is also well known that patients with PID often have complications such as autoimmune and allergic disorders.[1,3] Recently, the interaction between the immune and endocrine systems has been getting increasing attention.[4,5] However, there have so far been no reports focusing on the endocrine complications associated with PID in a large-scale survey.

Many endocrine disorders in patients with PID are thought to be due to the development of the autoimmunity, which is closely related to the pathophysiology of PID.[6] However, it is not known how the immunological and molecular defects in individual PID contribute to the development of various autoimmune endocrine disorders. In addition, the genetic defects in some PID can lead to these complications directly or indirectly via nonimmunological mechanisms.[6]

We analysed the endocrine complications in PID from the information obtained from the nationwide PID survey in Japan conducted in 2008. This is the first large-scale survey focusing on the endocrine complications in PID.

Materials and methods

This survey was performed according to the nationwide epidemiological survey manual of patients with intractable diseases (2nd edition 2006, Ministry of Health, Labour and Welfare of Japan) as described previously.[7] PID classification was based on the criteria of the International Union of Immunological Societies Primary Immunodeficiency Diseases Classification Committee in 2007.[8] The survey was conducted on patients with PID who were alive on 1 December 2008 and those who were newly diagnosed and died between 1 December 2007 and 30 November 2008 in Japan. The initial survey covered 1224 paediatric departments and 1670 internal medicine departments, which were randomly selected according to the number of beds among the 2291 paediatric departments and 8026 internal medicine departments in Japan. Primary questionnaires regarding the number of patients and the disease names based on the PID classification

Correspondence: Takafumi Nozaki, Department of Pediatrics, Graduate School of Medical Sciences, Kyushu University, 3-1-1 Maidashi, Higashi-ku, Fukuoka 812-8582, Japan. Tel.: +81 92 642 5421; Fax: +81 92 642 5435; E-mail: t-nozaki@pediatr.med.kyushu-u.ac.jp

were sent to the selected hospitals. The initial survey was conducted to investigate the prevalence of the respective PID. The secondary survey was performed to study the detailed clinical features of individual patients with PID. Secondary questionnaires regarding age, gender, clinical manifestations and complications other than those related to haematopoietic stem cell transplantation of individual patients with PID were sent to the respondents who answered that they observed at least one PID patient with characteristics listed in the primary questionnaires. The details of the methods of the questionnaire investigation, the response rates and the breakdown of the number of patients in both paediatric and internal medicine departments were described elsewhere.[9] The questionnaires were designed to elucidate the clinical characteristics including the manifestations and laboratory data of the patients. In this study, all endocrine manifestations in patients with PID were included as complications of PID, even if they were well known major symptoms of PID.

Results

Detailed clinical information was available from 923 (secondary survey) out of 1240 patients with PID (initial survey).[9] Among the 923 patients with PID, 49 (5·3%) had endocrine disorders. As shown in Table 1, more than two thirds of the patients with PID were <20 years old and the prevalence of endocrine diseases was much higher in the young population of patients with PID than that in the general young population,[7,10–14] even after excluding patients with immune dysregulation (PID category IV). As expected, hypoparathyroidism was the most common endocrine disorder, because it is very frequently observed in patients with DiGeorge syndrome. Endocrine manifestations were also common in patients with diseases of immune dysregulation, such as immune dysregulation, polyendocrinopathy, enteropathy, X-linked (IPEX) syndrome and autoimmune polyendocrinopathy-candidiasis-ectodermal dystrophy (APECED). Although the number of patients with defects in innate immunity was small, endocrine complications seemed to be more common than expected. Interestingly, endocrine disorders were not observed in patients with complement deficiencies. In addition, Graves' disease and Addison's disease were not observed in any of the patients with PID in this study.

Type 1 diabetes mellitus (T1D) was observed in six patients with PID (Tables 1 and 2) including four with type 1A (autoimmune) and two with type 1B (autoantibody-negative, idiopathic). Type 1A diabetes mellitus occurred frequently in patients with IPEX or IPEX-like syndrome (two of six patients, 33·3%) (Table 1). One patient of unknown aetiology in PID category IV showed type 1A diabetes and Hashimoto's thyroiditis along with recurrent viral infections (Tables 1, 2 and S1). In the cases of type 1A diabetes mellitus, anti-glutamic acid decarboxylase (GAD) autoantibodies and anti-insulin autoantibodies (IAA) were positive in all patients and in two of four patients, respectively (Table 2). The patients with IPEX and IPEX-like syndrome had a history of diabetic ketoacidosis with poor glycaemic control, and they developed T1D at a younger age than the other patients with PID. The first case of warts, hypogammaglobulinaemia, infections, and myelokathexis (WHIM) syndrome with T1D and hypothyroidism was included (Tables 2 and S2).[15] With regard to type 1B diabetes mellitus, the patient with hypogammaglobulinaemia of unknown aetiology had diabetic ketoacidosis (Table 2). On the other hand, type 2 diabetes mellitus (T2D) was observed in two patients with PID (Table 1).

Hashimoto's thyroiditis was observed in five patients with PID (Tables 1 and S1). The onset was very early in the patient with IPEX syndrome (at birth). All patients had at least 1 autoantibody among the anti-thyroid peroxidase (TPO), anti-thyroglobulin (Tg) and thyroid stimulating hormone receptor autoantibodies (TRAb).

Nonautoimmune hypothyroidism was reported in seven patients with PID (Tables 1 and S2). Anti-thyroid autoantibodies were all negative when measured. Among these, three patients with X-linked agammaglobulinaemia (XLA), IgG subclass deficiency or WHIM syndrome had primary (congenital) hypothyroidism detected by newborn mass screening. Hypothyroidism in the other four patients with normal TSH levels was considered to be due to central hypothyroidism, a disorder of the pituitary, hypothalamus or hypothalamic-pituitary portal circulation. Two patients with severe combined immunodeficiency (SCID) developed hypothyroidism before they received haematopoietic stem cell transplantation.

Growth hormone deficiency (GHD) was observed in six patients with PID (Tables 1 and S3), whose heights at the diagnosis of GHD ranged from −11·3 SD to −2·5 SD. Five patients were treated with growth hormone. One patient with SCID received cord blood transplantation when she was 20 months old, without conditioning chemotherapy or radiation.

Hypogonadism was observed in three patients with PID (Tables 1 and S4). Among them, two had hypergonadotrophic (primary) hypogonadism, whereas the other had hypogonadotrophic (central) hypogonadism. None of the patients received haematopoietic stem cell transplantation.

One common variable immunodeficiency disease (CVID) patient had isolated ACTH deficiency (Table 1). The other endocrine complications included hypophosphataemia, pseudohypoaldosteronism, adrenal crisis, hypoglycaemia and hypophosphataemic rickets as shown in Table 1.

Discussion

This is the first nationwide survey focusing on the endocrine complications of PID. Among these, hypoparathyroidism was the most common, observed in patients with DiGeorge syndrome and APECED.[16,17] In APECED, the calcium-sensing receptor has been reported to be the autoantigen responsible for hypoparathyroidism.[18] Although it has been reported that 79% of patients with APECED have hypocalcaemia due to hypoparathyroidism,[17] only 1 (25%) among four patients with APECED developed hypoparathyroidism in this study, which might be one of the clinical characteristics of patients with APECED in Japan.

The prevalence (33·3%) of T1D in patients with IPEX syndrome in this study seemed to be lower than that (>70%) of the previous reports.[19,20] The low prevalence of T1D might be due to